



**US Army Corps  
of Engineers**  
Waterways Experiment  
Station

Technical Report ITL-95-7  
September 1995

# Use of Reinforcement in a Nonlinear, Incremental Structural Analysis

*by Barry D. Fehl, Chris A. Merrill*



Approved For Public Release; Distribution Is Unlimited

19951031 148

DTIC QUALITY INSPECTED 5

Prepared for Headquarters, U.S. Army Corps of Engineers

The contents of this report are not to be used for advertising, publication, or promotional purposes. Citation of trade names does not constitute an official endorsement or approval of the use of such commercial products.



PRINTED ON RECYCLED PAPER

# Use of Reinforcement in a Nonlinear, Incremental Structural Analysis

by Barry D. Fehl, Chris A. Merrill

U.S. Army Corps of Engineers  
Waterways Experiment Station  
3909 Halls Ferry Road  
Vicksburg, MS 39180-6199

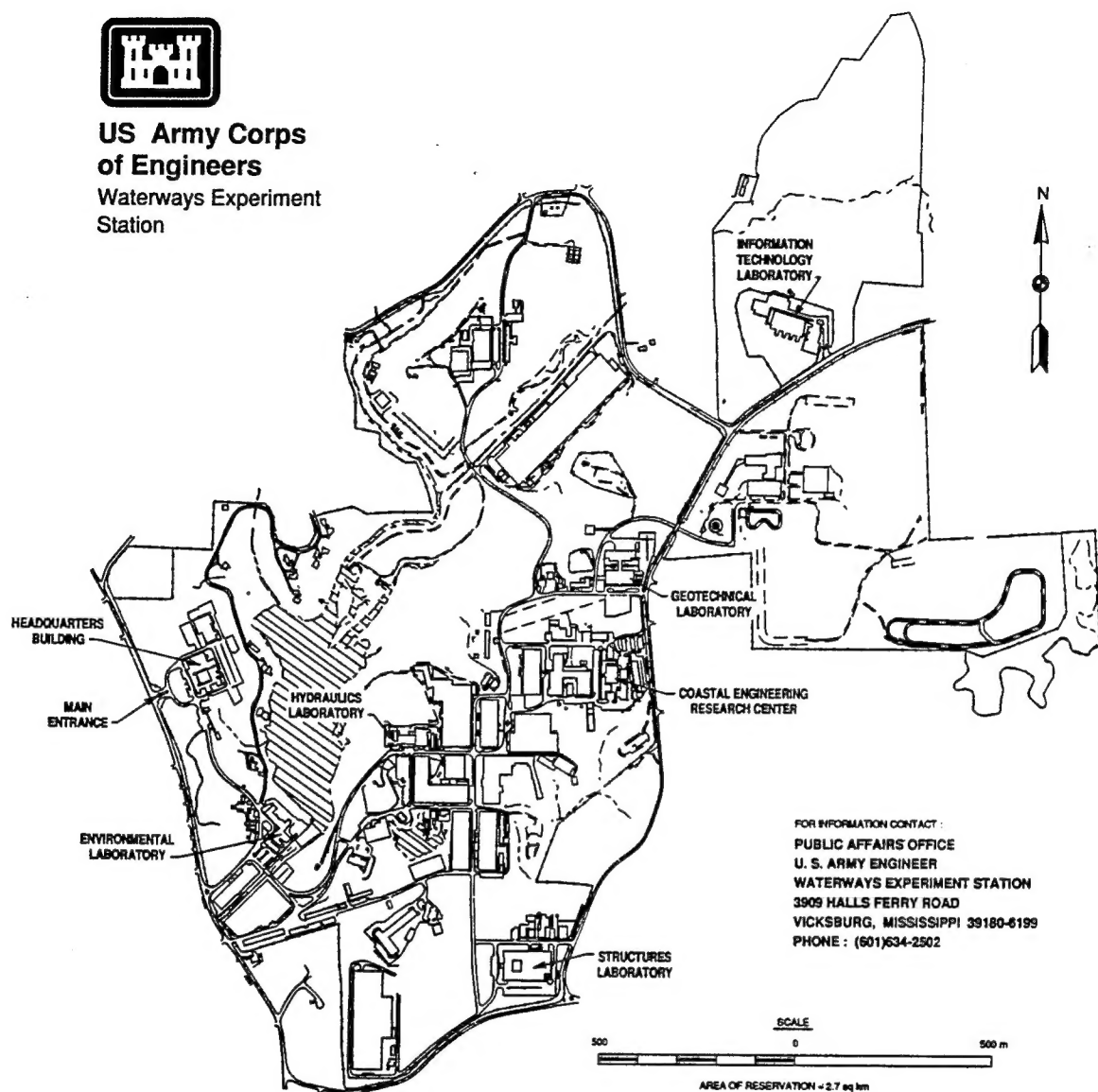
Accession For	
NTIS CRA&I	<input checked="" type="checkbox"/>
DTIC TAB	<input type="checkbox"/>
Unannounced	<input type="checkbox"/>
Justification .....	
By .....	
Distribution /	
Availability Codes	
Dist	Avail and/or Special
A-1	

Final report

Approved for public release; distribution is unlimited



**US Army Corps  
of Engineers**  
Waterways Experiment  
Station



FOR INFORMATION CONTACT :  
PUBLIC AFFAIRS OFFICE  
U. S. ARMY ENGINEER  
WATERWAYS EXPERIMENT STATION  
3909 HALLS FERRY ROAD  
VICKSBURG, MISSISSIPPI 39180-6199  
PHONE : (601)634-2502

**Waterways Experiment Station Cataloging-in-Publication Data**

Fehl, Barry D.

Use of reinforcement in a nonlinear, incremental structural analysis / by Barry D. Fehl,  
Chris A. Merrill ; prepared for U.S. Army Corps of Engineers.

74 p. : ill. ; 28 cm. -- (Technical report ; ITL-95-7)

Includes bibliographic references.

1. Structured analysis (Engineering) 2. Reinforcing bars. 3. Finite element method.  
I. Merrill, Chris A. II. United States. Army. Corps of Engineers. III. U.S. Army Engineer  
Waterways Experiment Station. IV. Information Technology Laboratory (U.S. Army  
Engineer Waterways Experiment Station) V. Title. VI. Series: Technical report (U.S. Army  
Engineer Waterways Experiment Station) ; ITL-95-7.

TA7 W34 no.ITL-95-7

# Contents

---

Preface .....	vii
Conversion Factors, Non-SI to SI Units of Measurement .....	viii
1—Introduction .....	1
Background .....	1
Purpose .....	3
Report Organization .....	4
2—Simple Beam Analyses .....	5
Introduction .....	5
Problem Formulation .....	5
Example Problems .....	12
Summary .....	17
3—Analyses of a Beam in Bending .....	18
Introduction .....	18
Problem Formulation .....	18
Example Problems .....	21
Summary .....	28
4—Analyses of a Slab .....	30
Introduction .....	30
Problem Formulation .....	30
Example Problems .....	34
Summary .....	41
5—Analyses of a Lock Chamber Monolith .....	42
Introduction .....	42
No Reinforcing Versus Reinforcing .....	43
Uncracked Versus Cracked .....	43
Summary .....	44

6—Summary and Conclusions .....	58
Summary .....	58
Conclusions .....	58
References .....	60
Appendix A: ABAQUS Modeling .....	A1
SF 298	

## List of Figures

---

Figure 1. Simple beam arrangements. a) Cantilever beam, b) Cantilever beam with an axial load, c) Fixed-fixed beam .....	7
Figure 2. Cantilever beam. a) Change in length due to decreased temperature, b) Equivalent change in length due to an applied axial load .....	8
Figure 3. Free body diagram of steel and concrete interaction for temperature change where $d$ is the height of the member .....	10
Figure 4. Free body diagram of steel and concrete interaction for mechanically applied load ( $p$ ). .....	11
Figure 5. Finite element mesh used with cantilever beam and fixed-fixed beam problems .....	13
Figure 6. Simply supported beam with loading to provide an area of constant moment .....	19
Figure 7. Free body diagram of half of the beam shown in Figure 6 .....	19
Figure 8. Graphic representation of a transformed section where $y'$ is the centroid of the transformed section .....	21
Figure 9. Simply supported beam geometry and loading .....	22
Figure 10. Finite element mesh for simply supported beam .....	23
Figure 11. Stress distribution through depth of beam for cracked and uncracked sections .....	26
Figure 12. Two-lift slab. a) Slab geometry, b) Unrestrained deflection of the slab subjected to the temperature gradient, c) Strain distribution for thermal loading shown in b .....	31

Figure 13. Strain distribution for a thermal loading of a two-lift slab . . . .	33
Figure 14. Finite element mesh of slab . . . . .	35
Figure 15. Transformed section of reinforced slab . . . . .	39
Figure 16. Reinforcing layout for chamber monolith at Olmsted Locks . .	42
Figure 17. Horizontal stress comparison of reinforced and unreinforced cases for element 493, integration point 1 . . . . .	45
Figure 18. Horizontal stress comparison of reinforced and unreinforced cases for element 763, integration point 3 . . . . .	46
Figure 19. Horizontal stress comparison of reinforced and unreinforced cases for element 756, integration point 3 . . . . .	47
Figure 20. Maximum principal stress comparison of reinforced and unreinforced cases for element 993, integration point 2 . . . . .	48
Figure 21. Maximum principal stress comparison of reinforced and unreinforced cases for element 1196, integration point 4 . . . . .	49
Figure 22. Horizontal stress comparison of cracked and uncracked cases for element 493, integration point 1 . . . . .	50
Figure 23. Horizontal stress comparison of cracked and uncracked cases for element 763, integration point 3 . . . . .	51
Figure 24. Horizontal stress comparison of cracked and uncracked cases for element 756, integration point 3 . . . . .	52
Figure 25. Maximum principal stress comparison of cracked and uncracked cases for element 993, integration point 2 . . . . .	53
Figure 26. Maximum principal stress comparison of cracked and uncracked cases for element 1196, integration point 4 . . . . .	54
Figure 27. Crack location plots. a) Left half of the model of the Olmsted chamber monolith, b) Right half of the model of the Olmsted chamber monolith . . . . .	55
Figure 28. Reinforcing stress comparison of cracked and uncracked cases for element 756 . . . . .	56
Figure 29. Reinforcing stress comparison of cracked and uncracked cases for element 763 . . . . .	57

Figure A1. Notations for identifying skewed reinforcement in an ABAQUS, eight-noded isoparametric element . . . . .	A2
Figure A2. Location of a reinforcing bar at midheight of an element . . . . .	A3

## List of Tables

---

Table 1. Length Change for Simple Beam Problem . . . . .	14
Table 2. Stresses for Simple Beam Problem (Fixed at Both Ends) . . . . .	14
Table 3. Stress in Concrete and Reinforcing for Cantilevered Beam Due to Temperature Change . . . . .	15
Table 4. Stress in Concrete and Reinforcing for Cantilevered Beam Due to Axially Applied Load . . . . .	16
Table 5. Stresses in Slab (Same Material in Both Lifts) . . . . .	36
Table 6. Stresses in Slab (Different Materials in Lifts) . . . . .	38
Table 7. Stresses in Slab with Reinforcing (Different Materials in Lifts) . . . . .	40



# Preface

---

The investigation described in this report was initiated as a part of Olmsted Locks Nonlinear, Incremental Structural Analysis (NISA) study and completed under the NISA work unit of the Structural Program of the Civil Works Research and Development (R&D) Program. The work was performed by the Computer-Aided Engineering Division (CAED), Information Technology Laboratory (ITL), U.S. Army Engineer Waterways Experiment Station (WES), Vicksburg, MS. Funds for publication of the report were provided from those available for the Computer-Aided Analysis of Massive Concrete Structures work unit of the Structural Program of the Civil Works R&D Program.

The investigation was accomplished under the general supervision of Dr. N. Radhakrishnan, Director, ITL, and under the direct supervision of Mr. H. Wayne Jones, Chief, CAED. This report was prepared by Messrs. Barry D. Fehl and Chris A. Merrill, CAED. The authors would like to acknowledge members of the Massive Concrete Structures CASE Committee who reviewed this report and provided comments.

At the time of publication of this report, Director of WES was Dr. Robert W. Whalin. Commander was COL Bruce K. Howard, EN.

*The contents of this report are not to be used for advertising, publication, or promotional purposes. Citation of trade names does not constitute an official endorsement or approval of the use of such commercial products.*

# Conversion Factors, Non-SI to SI Units of Measurement

---

Non-SI units of measurement used in this report can be converted to SI units as follows:

Multiply	By	To Obtain
degrees Fahrenheit	5/9	degrees Celsius or kelvins <sup>1</sup>
inches	25.4	millimeters
inch per inch per °F	0.5556	centimeters per centimeter per °C
pounds (mass)	0.4535924	kilograms
pounds (force) per inch	175.1268	newtons per meter
pounds (force) per square inch	0.006894757	megapascals
square inches	15.00064516	square meters
<sup>1</sup> To obtain Celsius (C) temperature readings from Fahrenheit (F) readings, use the following formula: $C = (5/9)(F - 32)$ . To obtain kelvin (K) readings, use $K = (5/9)(F - 32) + 273.15$ .		

# 1 Introduction

---

## Background

The evaluation of massive concrete structures for the effects of temperature has been part of the design process of these structures for many years. In recent years the evaluation of mass concrete structures has become more sophisticated, accounting for more parameters that affect the behavior of the structure, such as creep and shrinkage. Early evaluations were performed using hand calculations, but computers and associated software now make more sophisticated analyses possible.

In the late 1960's computer codes were developed for the Corps of Engineers by Dr. Edward Wilson of the University of California at Berkeley for the calculation of temperatures in a mass concrete structure and by R. S. Sandhu and others, also at Berkeley, for the calculation of stresses and strains resulting from gravity and thermal loads (Bombich, Norman, and Jones 1987). These finite element codes were used for the evaluation of Corps of Engineers projects until the middle 1980's.

During the design of the main lock for Locks and Dam No. 26 (Replacement), subsequently renamed Melvin Price Locks and Dam, a decision was made by the St. Louis District to investigate a state-of-the-art method for computing the stresses and strains in a massive concrete structure. The objective of this investigation was to develop a state-of-the-art tool for evaluating the main and auxiliary locks at Melvin Price Locks and Dam and to then use that tool to evaluate the structures for possible changes in construction procedures as cost savings measures.

In order to achieve the above objective, the St. Louis District contracted with the U.S. Army Engineer Waterways Experiment Station (WES) to perform a study to include the development of a state-of-the-art tool to be used to evaluate incrementally constructed mass concrete structures and to perform any analyses necessary on the Melvin Price Locks and Dam project. As part of this study, the general purpose finite element code ABAQUS (Hibbitt, Karlsson, and Sorensen 1994) was selected as the primary tool for performing the analyses. Using ABAQUS as the analytical tool, researchers developed procedures for modeling incremental construction of mass concrete structures. The inclusion of a constitutive model developed under the Repair, Evaluation, Maintenance, and Rehabilitation (REMR) Research Program completed the overall analytical process. The constitutive model included the capability to model the aging

characteristics of creep, shrinkage, and the modulus of elasticity and to predict cracking in the structure.

Once the procedures were established for performing the modeling, analyses were performed to evaluate several monoliths of the main and auxiliary locks at Melvin Price Locks and Dam. The results of the analyses performed were reported in four different reports:

- “Thermal Stress Analyses of Mississippi River Lock and Dam 26(R)” (Bombich, Norman, and Jones 1987),
- “Evaluation of Thermal and Incremental Construction Effects for Monoliths AL-3 and AL-5 of the Melvin Price Locks and Dam” (Truman, Petruska, and Ferhi 1992),
- “Refined Stress Analysis of Melvin Price Locks and Dam” (Jones 1992),
- “Evaluation of Parameters Affecting Thermal Stresses in Mass Concrete” (Bombich, Garner, and Norman 1991).

The culmination of these efforts was a study that evaluated the lift heights in some of the more massive lock monoliths. The results indicated that increased lift heights in these monoliths would not significantly increase the potential for cracking. Based on these results, the lift heights were increased in four monoliths—resulting in a construction cost savings of \$1.2 million.

Following the study on Melvin Price Locks and Dam, WES was contracted by the Vicksburg District to evaluate Lock and Dam Nos. 4 and 5 on the Red River. Using the tools and procedures developed in the Melvin Price Locks and Dam study, WES researchers analyzed Red River Lock and Dam Nos. 4 and 5 and made recommendations on lift heights, placement temperatures, and insulation. The complete description of the analyses and results are presented in “Red River Thermal Studies, Report 2, Thermal Stress Analyses” (Garner, Hammons, and Bombich 1991).

At about the same time the analyses of the Red River projects were being performed, Engineer Technical Letter (ETL) 1110-2-324 “Special Design Provisions for Massive Concrete Structures” was being developed (Headquarters, U.S. Army Corps of Engineers 1990). Development of ETL 1110-2-324 relied primarily on the studies performed for Melvin Price Locks and Dam. The ETL was written to provide official guidance for the performance of nonlinear, incremental structural analysis (NISA) of massive concrete structures and to ensure consistency in the evaluation of massive concrete structures.

Subsequent to the analyses of the Red River projects and the publication of ETL 1110-2-324, a series of studies on the Olmsted Locks and Dam was undertaken by WES for the Louisville District. Using the guidelines provided by ETL 1110-2-324 and developing new guidelines (in coordination with Headquarters, U.S. Army Corps of Engineers) for portions of the NISA process not covered in the ETL, WES evaluated different concrete mixtures, concrete

placing schemes, placement temperatures, insulation requirements, and constructability of several lock monoliths from the Olmsted project.

Due to the magnitude of the study for the Olmsted project, the NISA process was able to progress and improve during the course of the study. Prior to the Olmsted project, three-dimensional (3-D) analysis had been very limited. However, acquisition of a CRAY-YMP supercomputer significantly improved the capability for performing large 3-D analyses. The supercomputer allowed several 3-D analyses to be performed and was of great importance in understanding the structural behavior of several monoliths. In addition, the ability to graphically display the locations of cracking was included during the course of the study and the capability to create plots showing contours of the levels of stress and strain as percentages with respect to the failure criteria. During the course of the study the procedures for including reinforcement were developed and were implemented in some of the analyses. The preparatory work leading to modeling reinforcement in a NISA is presented in this report.

The various studies performed for the Olmsted NISA are well documented in a set of reports. These reports are:

- "Nonlinear, Incremental Structural Analysis of Olmsted Locks and Dam, Volume I, Main Text" (Garner et al. 1992),
- "Nonlinear, Incremental Structural Analysis of Olmsted Locks: Phase III" (Merrill, Fehl, and Garner 1995),
- "Three-Dimensional, Nonlinear, Incremental Structural Analysis of a Culvert Valve Monolith Wall, Olmsted Locks" (Fehl and Merrill, in preparation),
- "Nonlinear, Incremental Structural Analysis for the Lower Miter Gate Monolith at Olmsted Locks and Dam" (Fehl et al., in preparation).

ETL 1110-2-324 was updated to include the lessons learned from the Olmsted study. ETL 1110-2-365, "Nonlinear, Incremental Structural Analysis of Massive Concrete Structures," published 31 August 1994, provides guidance for evaluating massive concrete structures and includes the advances made in studies that have been performed to date.

## Purpose

The primary purpose of this report is to develop a basic understanding of how stresses and strains in reinforcing and concrete can be computed using conventional techniques and how well these values can be compared to results of a NISA-type analysis. The approach used begins by looking at simple problems and performing the computations both by hand and numerically. The hand calculations will show the process used when steel reinforcing is included in the analysis, and the numerical solution will be compared to the hand solution to produce confidence in the numerical solution. The development of procedures to

model reinforcement in a NISA will culminate with a demonstration of how to implement reinforcing into an ABAQUS finite element model of a lock monolith.

Since a NISA provides a prediction of cracking which may occur, including reinforcing in the analysis can be very important. If cracking is not considered, then inclusion of steel reinforcing in a NISA would provide little benefit since the load carried by the reinforcement is small until a crack occurs. Once a crack does occur, stresses in the reinforcement at the crack location rise dramatically and can become quite high.

Inclusion of reinforcement may not appear to be an important issue for massive concrete structures since these types of structures are stereotyped as having little if any reinforcement. There is at least some reinforcement in most Corps of Engineers mass concrete structures, with the exception of structures constructed using roller-compacted concrete. Since steel reinforcing is present in most massive concrete structures built by the Corps of Engineers, the fact that the reinforcement is present should be accounted for in analyses performed since the NISA process is an attempt to predict the actual behavior of the structure.

## **Report Organization**

As mentioned previously, a progressive approach will be taken in presenting the use of reinforcement in a NISA. The initial problem will be of a simple beam with temperature and mechanical loads applied and with varying support conditions to show how stresses and displacements are computed in the concrete and the reinforcing. The second problem presented will be a simply supported beam loaded to show how the reinforcing behaves in bending. The final simplified problem will be a slab with two lifts and a temperature gradient applied through the thickness of the slab to demonstrate behavior in a slab from a thermally induced load which produces a bending mechanism.

The final sections of the report will present results from an analysis performed during the Olmsted Locks NISA study which included reinforcement. Also, a presentation will be made which shows how to implement reinforcing into a finite element model using the ABAQUS code. Finally, conclusions and recommendations from work reported herein as well as from other sources will be provided along with helpful suggestions for avoiding problems when using reinforcement in a model.

## 2 Simple Beam Analyses

---

### Introduction

For most designs performed by a structural engineer the effects of temperature are neglected. While almost every structure will undergo changes due to temperature loads, for most structures the loads produced by temperature changes are small compared to the service loads applied. This is not necessarily the case for massive concrete structures where the loads due to changes in temperature can be the most severe loads applied. Because many structural engineers do not have a significant amount of experience in dealing with temperature loadings, part of the objective of the simple examples presented in this chapter is to explain how temperature changes affect a structure.

When a solid body undergoes a temperature change, the result is a change in the volume of that body. For most solids, if the temperature in the body drops, the volume will decrease; and if the temperature rises, the volume will increase. Depending on the restraint conditions on a body undergoing a temperature change, there may or may not be stresses associated with the volume change which occur as a result of this temperature change. If the body is completely unrestrained, then no stresses will result due to changes in temperature. The maximum stresses possible will occur due to changes in temperature if the body is being fully restrained. Therefore, the level of stress a body will experience is a function of the change in temperature and the amount of restraint present.

### Problem Formulation

#### Unreinforced problem

For the case of an unrestrained body, the change in volume due to a temperature change is a function of the geometry of the body, the magnitude of the temperature change, and the coefficient of thermal expansion. The coefficient of thermal expansion is a material property. For concrete, the value can vary from one mixture to another, but is usually between  $4 \times 10^{-6}$  in./in./°F and  $6 \times 10^{-6}$  in./in./°F.<sup>1</sup> For the purpose of demonstrating changes due to temperature, consider the one-dimensional (1-D) case of a cantilever beam as

---

<sup>1</sup> A table of factors for converting non-SI units of measurement to SI units is presented on page viii.

shown in Figure 1a. If this beam is subjected to a uniform temperature change, the change in length due to the change in temperature is computed by

$$\Delta L = \alpha L(\Delta T) \quad (1)$$

where

$\Delta L$  = change in length  
 $\alpha$  = coefficient of thermal expansion  
 $L$  = length of member  
 $\Delta T$  = change in temperature

The resulting change in length due to a change in temperature can be obtained through the application of an equivalent mechanical load as well. To demonstrate how this equivalent load can be computed, the 1-D case is again used. For the 1-D case, an axial load must be applied at the free end of the cantilever beam shown in Figure 1b. The equation for a change in length due to an applied axial load is:

$$\Delta L = \frac{PL}{AE} \quad (2)$$

where

$P$  = equivalent mechanical load  
 $A$  = cross-sectional area of member  
 $E$  = modulus of elasticity of material

Using the expression in Equation 1 for  $\Delta L$  and substituting this expression for  $\Delta L$  into Equation 2 and solving for  $P$  results in:

$$P = \frac{AE\alpha L(\Delta T)}{L}$$

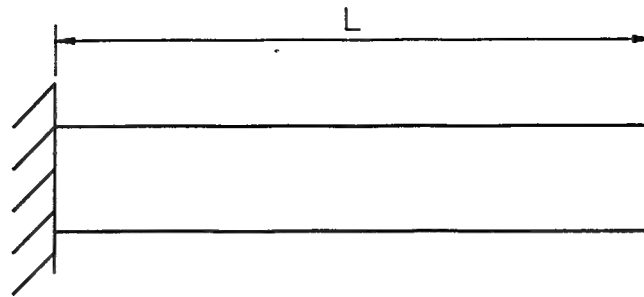
If the length term is cancelled, the expression for the equivalent mechanical load  $P$  which would produce the same displacement as was produced by the change in temperature may be obtained.

$$P = AE\alpha(\Delta T) \quad (3)$$

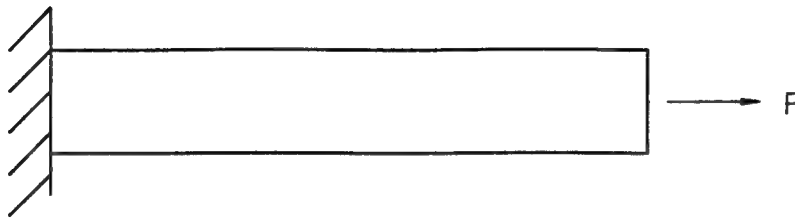
Now consider the same beam but with a fixed support added at the free end of the beam as shown in Figure 1c. Again, assume it is subjected to a uniform change in temperature of  $\Delta T$ . Since it can no longer displace due to it being fixed at both ends, then a stress within the beam will be introduced instead of a change of length.

The equivalent mechanical load can be used to help explain the stresses which occur in the beam due to the temperature change. As shown in Figure 2a, the beam when it undergoes the decrease in temperature wants to reduce in length by a distance  $\Delta L$  as determined by Equation 1. Now, if the equivalent mechanical

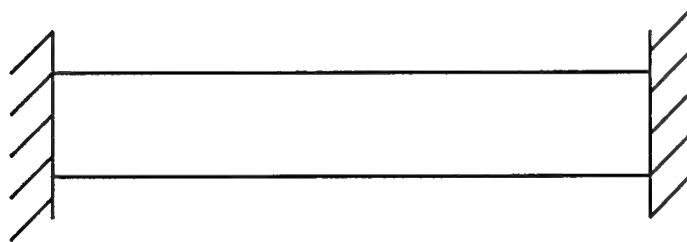




a. Cantilever beam



b. Cantilever beam with an axial load



c. Fixed-fixed beam

Figure 1. Simple beam arrangements

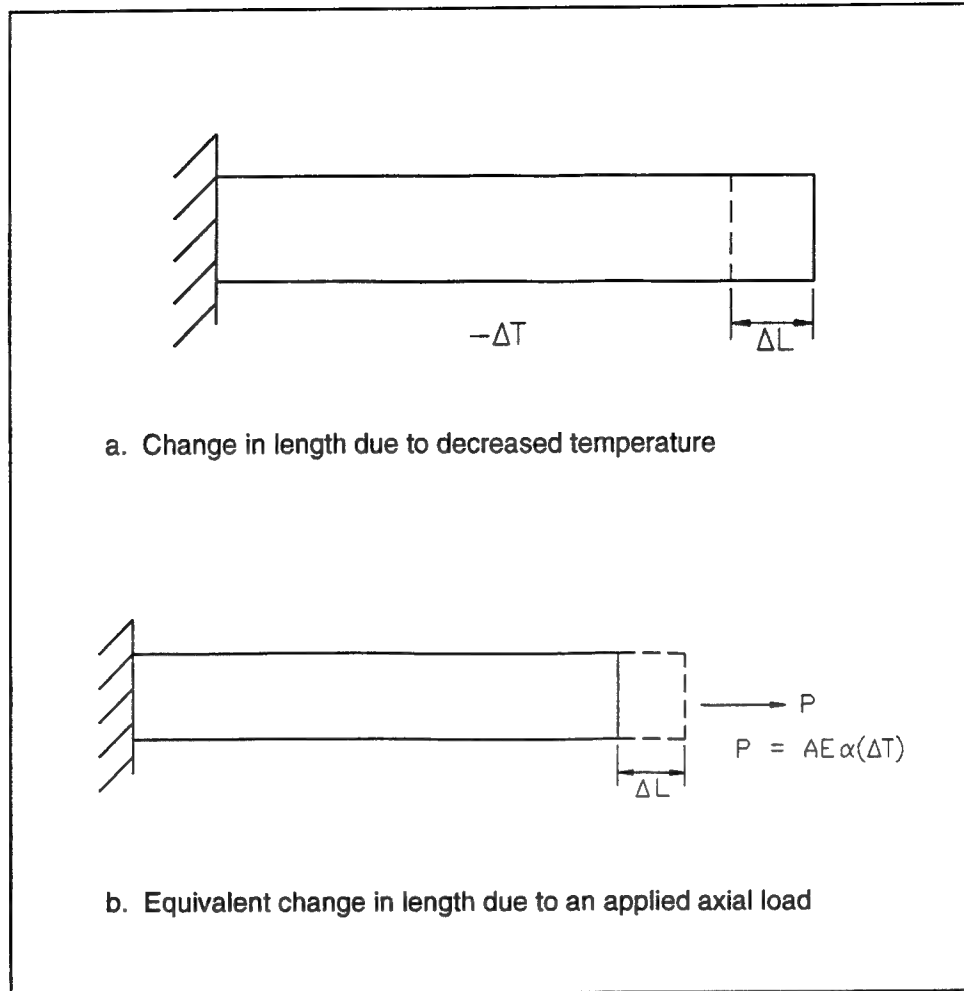


Figure 2. Cantilever beam

load, as computed using Equation 3, is applied such that the change in length it will produce is opposite to the change in length created by the temperature decrease, then the load will produce the same stress in the beam as would be seen in a fixed-fixed beam undergoing the temperature decrease. For the case of a decrease in temperature, the equivalent mechanical load can be applied as shown in Figure 2b to produce the tension in the beam that would occur due to the temperature change.

The stress in the fixed-fixed beam due to a change in temperature could also be calculated directly. Since it is known that for an axially loaded beam that

$$\sigma = \frac{P}{A} \quad (4)$$

then substituting the expression for  $P$  as given Equation 3 results in

$$\sigma = -[E\alpha(\Delta T)] \quad (5)$$

## Reinforced problem subjected to temperature loading

Reinforcement is present in most concrete structures including massive concrete structures. Since reinforcement is included to provide tensile strength to a structure and to limit cracking, excluding reinforcing which is present in a structure from a numerical model used to analyze that structure is conservative. While in some cases not including reinforcing in the model used to perform a NISA may be acceptable, in many cases neglecting the presence of the reinforcing could lead to a design that is not economical or to a conclusion that the structure has severe cracking problems when in fact the presence of reinforcing will reduce the extent of cracking which occurs. This portion of the chapter describes how reinforcing affects a simple concrete member.

First consider the cantilever beam as shown before in Figure 1a but now assume that there is a reinforcing bar in the concrete. If the beam is subjected to a uniform temperature change, the concrete and steel will have a change in length due to this temperature change. If this temperature change was applied to each material independently, the change in length for each material would be

$$\Delta L_C = \alpha_C L \Delta T \quad (6)$$

$$\Delta L_S = \alpha_S L \Delta T \quad (7)$$

where the subscript "C" refers to concrete and the subscript "S" refers to steel. For the case where the coefficient of thermal expansion for concrete is different from the coefficient of thermal expansion of the steel, a force will build between the concrete and the steel as the temperature changes since the rate of change in length is different for the two materials. The method used to model reinforcing in a NISA assumes no bond slippage, so the force building at the steel/concrete interface can be described by the free body diagram in Figure 3. Summing the forces in the horizontal direction results in

$$P_C + P_S = 0 \rightarrow P_S = -P_C \quad (8)$$

Since an internal force is induced on the beam, then the total changes in length are a function of both the temperature as described in Equations 6 and 7 above and the internal force as based on Equation 2. Therefore, the total change in length for the concrete ( $\Delta L_C$ ) and the steel ( $\Delta L_S$ ) can be computed by adding the components of change in length due to temperature and the internal force ( $P_C$  and  $P_S$ ) as follows:

$$\Delta L_C = \alpha_C L \Delta T + \frac{P_C L}{A_C E_C} \quad (9)$$

$$\Delta L_S = \alpha_S L \Delta T + \frac{P_S L}{A_S E_S} \quad (10)$$

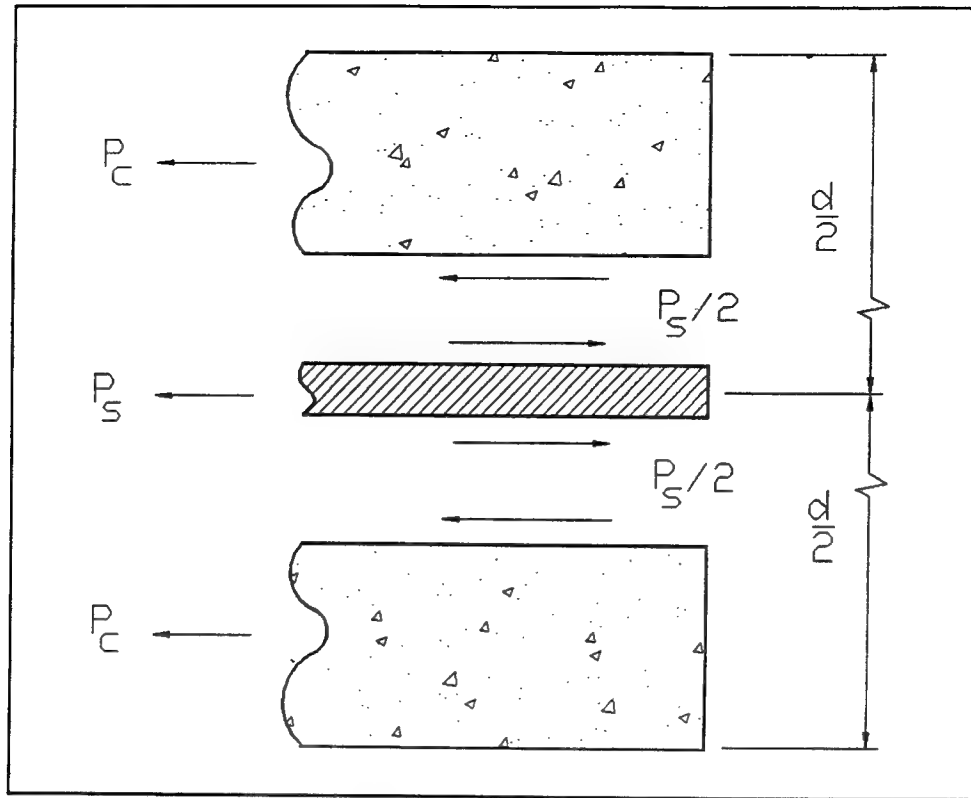


Figure 3. Free body diagram of steel and concrete interaction for temperature change where  $d$  is the height of the member

Now, since full bond between the concrete and the steel is assumed, then there must be compatibility between the changes in length. This compatibility is defined by

$$\Delta L = \Delta L_C = \Delta L_S \quad (11)$$

Substituting Equations 9 and 10 into Equation 11 and using Equation 8 for  $P_S$  results in

$$\alpha_C L \Delta T + \frac{P_C L}{A_C E_C} = \alpha_S L \Delta T - \frac{P_C L}{A_S E_S}$$

Solving for  $P_C$  gives

$$P_C = \frac{\Delta T (\alpha_S - \alpha_C)}{\left( \frac{1}{A_C E_C} + \frac{1}{A_S E_S} \right)} \quad (12)$$

So the force acting on the concrete due to the change in temperature is  $P_C$  and from Equation 8,  $P_S$  is equal to  $P_C$  but acting in the opposite direction as seen in

Figure 4. These are the equivalent mechanical loads developed in the concrete and reinforcing and can be used to compute the stresses using Equation 4.

### Reinforced problem subjected to axial load

The final problem that will be examined in this chapter is a reinforced cantilevered beam subjected to an axial force applied at the free end of the beam. Unlike the previous reinforced beam example, the total force in the concrete is summed with the total force in the steel to obtain the total force  $P$  acting on the beam. So

$$P = P_C + P_S \quad (13)$$

Using Equation 2 and rearranging terms, the forces for the concrete and the steel can be calculated by

$$P_C = \frac{(\Delta L_C) A_C E_C}{L} \quad (14)$$

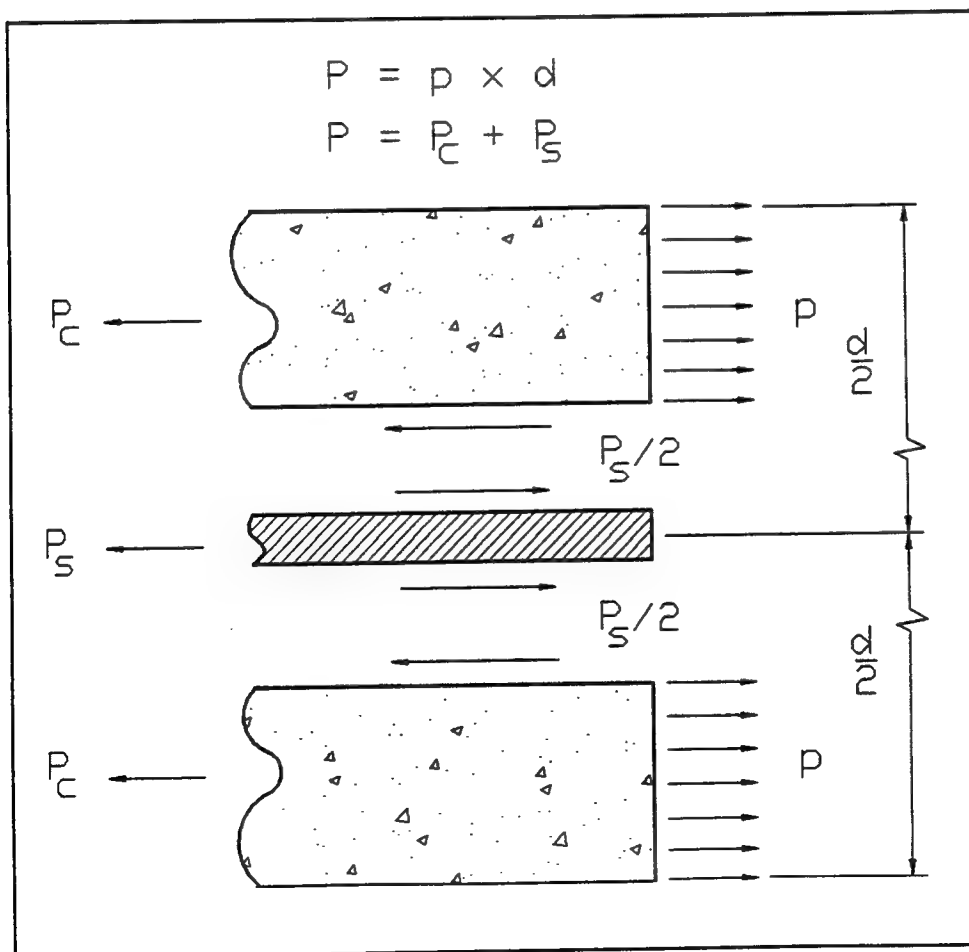


Figure 4. Free body diagram of steel and concrete interaction for mechanically applied load ( $P$ )

$$P_s = \frac{(\Delta L_s) A_s E_s}{L} \quad (15)$$

Substituting these two expressions into Equation 13, the following expression for the total force  $P$  can be obtained.

$$P = \frac{A_c E_c}{L} (\Delta L_c) + \frac{A_s E_s}{L} (\Delta L_s) \quad (16)$$

As in the previous reinforced beam problem though, compatibility between the concrete and the steel reinforcing must be maintained as shown in Equation 11. Therefore,  $\Delta L$  can replace  $\Delta L_c$  and  $\Delta L_s$ . Making this substitution and solving for  $\Delta L$  results in

$$\Delta L = \frac{PL}{(A_c E_c + A_s E_s)} \quad (17)$$

which is the change in length of the beam due to the applied force  $P$ . Now, since

$$\sigma = \frac{P}{A}$$

and substituting Equations 14 and 15 into this equation for stress, the stress can be computed as follows:

$$\sigma_c = \frac{\Delta L (E_c)}{L} \quad (18)$$

$$\sigma_s = \frac{\Delta L (E_s)}{L} \quad (19)$$

These equations give the capability of computing the stress in the concrete and the steel due to an axial load  $P$ .

## Example Problems

In order to better understand how to apply the above equations, examples are presented below to show how the equations are used when real values are assigned to the various parameters. Besides showing the process of the calculations, the examples will show the magnitude of the equivalent mechanical load when compared to its corresponding temperature change and the extent that including reinforcing affects the results. In addition, the hand solutions will be compared to numerical solutions.

### Simple beam - no reinforcing included

Consider the cantilever beam shown in Figure 1a. Now, if the beam is assumed to be 72 in. long and to have a unit thickness with a coefficient of thermal expansion of  $4.0 \times 10^{-6}$  in./in./°F, a modulus of elasticity of  $4.0446 \times 10^6$  psi, and is subjected to a uniform drop in temperature of 20 °F, then the change in length of beam due to the temperature drop can be computed using Equation 1:

$$\Delta L = (4.0 \times 10^{-6} \text{ in./in./°F})(72 \text{ in.})(-20 \text{ °F})$$

$$\Delta L = -0.00576 \text{ in.}$$

Similarly, using Equation 3, the equivalent mechanical load can be computed:

$$P = (12 \text{ in.}^2)(4.0446 \times 10^6 \text{ psi})(4.0 \times 10^{-6} \text{ in./in./°F})(-20 \text{ °F})$$

$$P = -3882.8 \text{ lb}$$

So if a temperature decrease of 20 °F is uniformly applied to the beam shown in Figure 1a or a compressive force equivalent to 3882.8 lb is applied to the end of the beam, the resulting decrease in length will be 0.00576 in. This should agree with numerical results as well. Using the finite element mesh shown in Figure 5 and the finite element code, ABAQUS, a numerical analyses will be performed on the beam shown in Figure 1 for both the case of the drop in temperature and the applied mechanical load. The results from the finite element analyses are shown in Table 1, and, as can be seen, the results are exactly the same as the hand calculations shown above.

Now apply the 20 °F temperature drop to the fixed-fixed beam case and the resulting stress can be computed directly using Equation 5:

$$\sigma = -[(4.0446 \times 10^6 \text{ psi})(4.0 \times 10^{-6} \text{ in./in./°F})(-20 \text{ °F})]$$

$$\sigma = 323.6 \text{ psi}$$

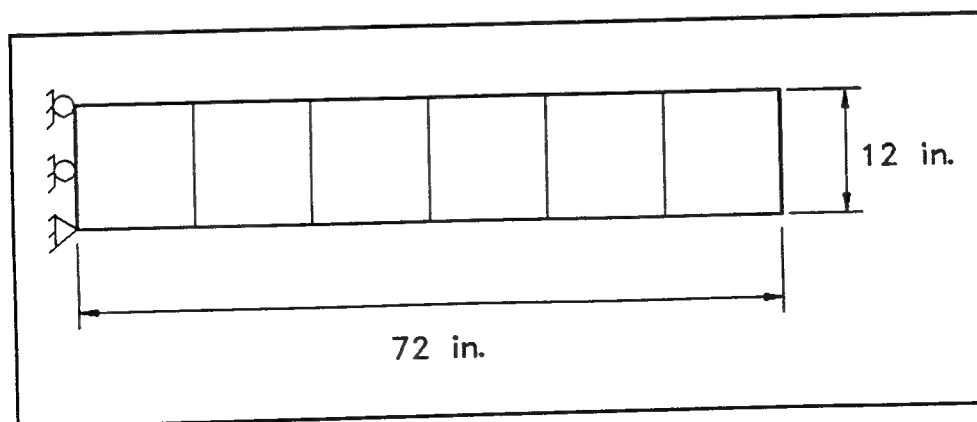


Figure 5. Finite element mesh used with cantilever beam and fixed-fixed beam problems

**Table 1**  
**Length Change for Simple Beam Problem**

Type of Load	Change in Beam Length, in.	
	Hand Solution	ABAQUS Solution
20 °F temp. drop	-0.00576	-0.00576
3882.8-lb force	-0.00576	-0.00576

Alternately, the stress in the beam can be computed by using the equivalent mechanical load computed above and Equation 4:

$$\sigma = \frac{3882.8 \text{ lb}}{12 \text{ in.}^2}$$

$$\sigma = 323.6 \text{ psi}$$

Again the solution of this problem can be checked numerically using ABAQUS. An analysis was performed for the fixed-fixed beam subjected to a 20°F temperature drop and a cantilever beam subjected to an axial tension load of 3882.8 lb. The results of those analyses as compared to the hand solutions are shown in Table 2 and, as before, the numerical and hand solutions are exactly the same.

**Table 2**  
**Stresses for Simple Beam Problem (Fixed at Both Ends)**

Type of Load	Stress in Beam, psi	
	Hand Solution	ABAQUS Solution
20 °F temp. drop	323.6	323.6
3882.8-lb force	323.6	323.6

### Simple beam—reinforcement included

The equations for the beam with a reinforcing bar included can now be implemented for the cantilevered beam case shown in Figure 1a. As for the unreinforced case, the temperature change is a 20°F drop, and the area, the modulus of elasticity, and the coefficient of thermal expansion for the concrete are as were defined previously. The beam under consideration is assumed to be 12 in. wide with a single #9 reinforcing bar ( $A_s = 1.0 \text{ in.}^2$ ) in the center. Since a unit thickness is used in the analytical solution the area of the reinforcing is  $0.083 \text{ in.}^2$  ( $A_s/12 \text{ in.}^2$ ). The modulus of elasticity for steel of  $29.0 \times 10^6 \text{ psi}$  will be used and a coefficient of thermal expansion of  $6.5 \times 10^{-6} \text{ in./in./}^\circ\text{F}$ . The force in the concrete  $P_c$  can then be computed as follows from Equation 12:



$$P_C = \frac{(-20 \text{ }^{\circ}\text{F})(6.5 \times 10^{-6} \text{ in./in./}^{\circ}\text{F} - 4.0 \times 10^{-6} \text{ in./in./}^{\circ}\text{F})}{\frac{1}{(12 \text{ in.}^2)(4.0446 \times 10^6 \text{ psi})} + \frac{1}{(0.083 \text{ in.}^2)(29.0 \times 10^6 \text{ psi})}}$$

$$P_C = -114.7 \text{ lb}$$

and from Equation 8, the force  $P_S$  in the steel can be obtained,

$$P_S = -P_C = 114.7 \text{ lb}$$

Using the equation from mechanics for stress in a pure tension member, the stress in the concrete and the reinforcing can be computed as follows:

$$\sigma_C = \frac{P_C}{A_C} = \frac{-114.7 \text{ lb}}{12 \text{ in.}^2}$$

$$\sigma_C = -9.56 \text{ psi}$$

$$\sigma_S = \frac{P_S}{A_S} = \frac{114.7 \text{ lb}}{0.083 \text{ in.}^2}$$

$$\sigma_S = 1382 \text{ psi}$$

So the stress in the steel is much higher than the stress in the concrete but it is still well below the yield strength of 60,000 psi of typical reinforcing bars.

As before, the hand calculations can be compared to calculations from a numerical analysis. For the case with reinforcing, two separate finite element analyses were performed. The first finite element analysis used a capability contained in ABAQUS which allows the user to define the size and location of a reinforcing bar in an element and then the stiffness of the reinforcing bar is incorporated into the overall stiffness of the model. The second finite element analysis will employ the use of truss elements connected to the midside nodes of the beam to model the reinforcing bars. The results are compared in Table 3. As can be seen, the steel stresses are in exact agreement while for the concrete stresses the two numerical solutions agree well but are slightly different from the stress computed by hand.

<b>Table 3</b> <b>Stress in Concrete and Reinforcing for Cantilevered Beam Due to Temperature Change</b>		
Type of Solution	$\sigma_C$ , psi	$\sigma_S$ , psi
Hand calculation	-9.56	1,382
ABAQUS - REBAR elem.	-9.60	1,382
ABAQUS - Truss elem.	-9.60	1,382

The two different methods of modeling reinforcement are used to show that the method of reinforcement modeling will not affect the results. The truss element is included because it is the method that was used prior to acquiring the ability to model reinforcing as part of the continuum element. In addition, there are still finite element programs which do not have the reinforcement modeling capability of ABAQUS. Since the ABAQUS method of modeling reinforcing is the technique used in NISA, it is important to understand that it will produce the same results as if the reinforcement is modeled discretely with a truss element. The ABAQUS reinforcement modeling capabilities will be discussed further in Appendix A.

Finally, the use of Equations 17-19 can be demonstrated by using the equivalent mechanical load applied previously to the unreinforced beam. This load was 3882.8 lb. First, using Equation 17, the change in length due to the load is computed.

$$\Delta L = \frac{(3882.8 \text{ lb})(72 \text{ in.})}{(12 \text{ in.}^2)(4.0446 \times 10^6 \text{ psi}) + (0.083 \text{ in.}^2)(29.0 \times 10^6 \text{ psi})}$$

$$\Delta L = 0.00549 \text{ in.}$$

This change in length can now be used to compute the stresses in the concrete and the reinforcing.

$$\sigma_c = \frac{(0.00549 \text{ in.})(4.0446 \times 10^6 \text{ psi})}{72 \text{ in.}}$$

$$\sigma_c = 308.4 \text{ psi}$$

$$\sigma_s = \frac{(0.00549 \text{ in.})(29.0 \times 10^6 \text{ psi})}{72 \text{ in.}}$$

$$\sigma_s = 2211.3 \text{ psi}$$

Table 4 compares these stresses to those computed using ABAQUS. The results from the three separate calculations are all very close, but as with the previous example which included reinforcing, there are small differences between the hand solutions and the ABAQUS solutions.

<b>Table 4</b> <b>Stress in Concrete and Reinforcing for Cantilevered Beam Due to Axially Applied Load</b>		
<b>Type of Solution</b>	<b><math>\sigma_c</math>, psi</b>	<b><math>\sigma_s</math>, psi</b>
Hand calculation	308.4	2,211
ABAQUS - REBAR elem.	308.2	2,212
ABAQUS - Truss elem.	308.2	2,212

## Summary

The above discussion has shown how temperature can affect a structure such as a beam with basic support conditions. Simple examples are convenient to demonstrate how computation of stresses and displacements are accomplished for cases of temperature loading. In addition, the magnitude of temperature loadings can be gauged through the use of equivalent mechanical loads which allows comparison of a temperature loading to a physical load with which the reader may be more familiar.

The discussion in this chapter also showed that methods used for computing stresses in the finite element code ABAQUS can be checked and verified against hand solutions for cases with and without reinforcing. The purpose of such comparisons for simple problems is to provide confidence in the code and modeling techniques which can be applied to more complicated problems where hand solutions are not possible.

# 3 Analyses of a Beam in Bending

---

## Introduction

Now that demonstrations of how a finite element analysis can predict stresses in unreinforced and reinforced beams for both a temperature load and an axial load have been shown, the next step is to look at another type of mechanical loading. A simply supported beam will be used to show how stresses are computed for a bending mechanism for both a reinforced and an unreinforced case. The approach in showing these calculations will be similar to that used in Chapter 2 for the temperature and axial loadings.

## Problem Formulation

The beam that will be used for the calculations will be loaded as shown in Figure 6. This type of loading is used so that a region of constant moment and zero shear can be achieved. The geometry and loading were selected to match classic beam theory assumptions used to derive the hand calculation techniques.

Before calculations of stress can be performed, the moment which creates the stresses in the beam must be determined. The moment used for the problems in this report will be derived but solutions can be found in various other references. The problems evaluated will investigate the stresses in the region of constant moment. To calculate the moment in the center portion of the beam, use the free body diagram of the left portion of the beam as shown in Figure 7. From statics it is known that summing the moments about any point will be equal to zero, so if the moments are summed about point *B* in Figure 7, the resulting equation is:

$$P_x - pa(x - a/2) - M = 0$$

Substituting  $pa$  for the reaction  $P$  and solving for  $M$  gives:

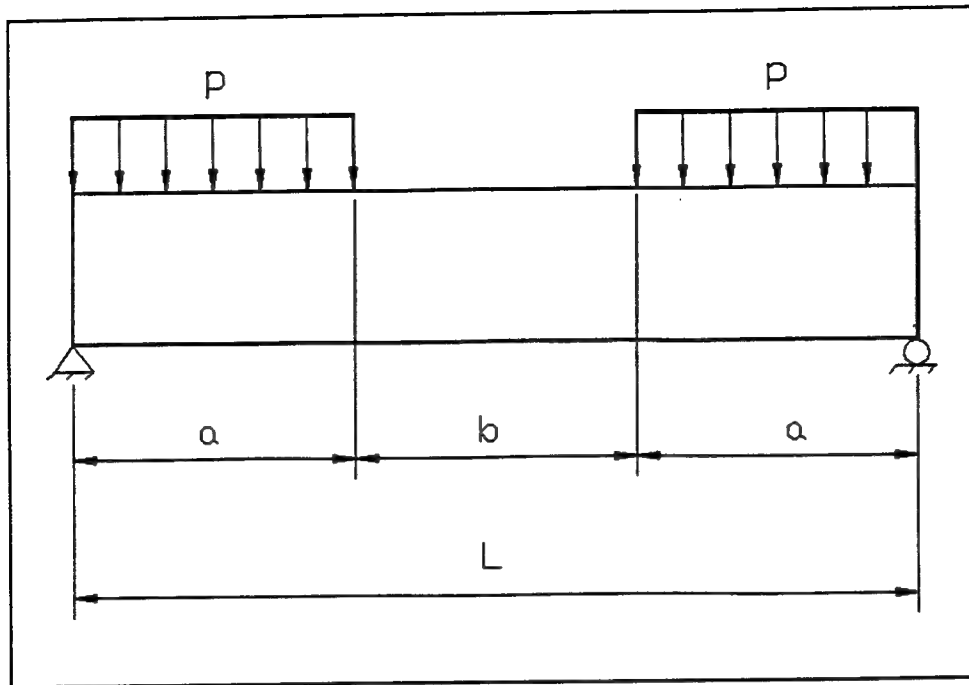


Figure 6. Simply supported beam with loading to provide an area of constant moment

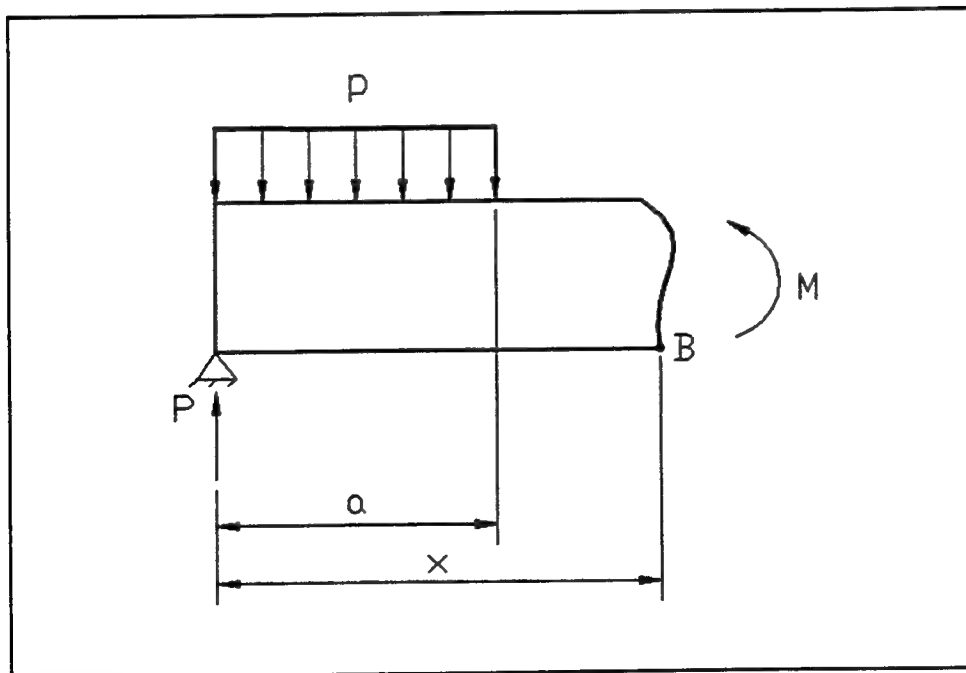


Figure 7. Free body diagram of half of the beam shown in Figure 6.

$$\begin{aligned}
 M &= P_x - pa(x - a/2) \\
 &= \frac{pax - pax + (pa^2)}{2} \\
 &= \frac{pa^2}{2}
 \end{aligned}
 \tag{21}$$

which provides the moment which can be used to calculate the stresses in the subsequent problems.

### Unreinforced problem

For the case of the unreinforced beam, the calculation of stress at any point through the depth of the beam is given by:

$$\sigma = \frac{-My}{I} \tag{22}$$

where

$M$  = moment in the beam

$y$  = distance from the neutral axis of the beam to the point where the stress is to be determined

$I$  = moment of inertia of the beam cross section

### Reinforced problem

Inclusion of reinforcing into the problem requires the method of transformed sections to be used to obtain the stresses in both the concrete and the reinforcing. Using a ratio of the steel modulus to the concrete modulus  $n$ , the area of the steel reinforcing can be converted into an equivalent area of concrete so that the problem can be analyzed as a single material. This transformation of areas is graphically demonstrated in Figure 8.

Once the transformed section has been determined, the neutral axis and the moment of the inertia of the transformed section must be computed since the neutral axis is no longer at the midheight of the beam. Once these parameters have been computed, the stress in the concrete at any location through the depth of the beam can be computed using Equation 21. To compute the stress in the steel requires first that the stress in concrete be computed at the location of the steel and then multiplying this stress by the ratio of the steel modulus to the concrete modulus. In equation form, the steel stress is:

$$\sigma_s = n \sigma_c \tag{23}$$

where

$\sigma_s$  = stress in reinforcing

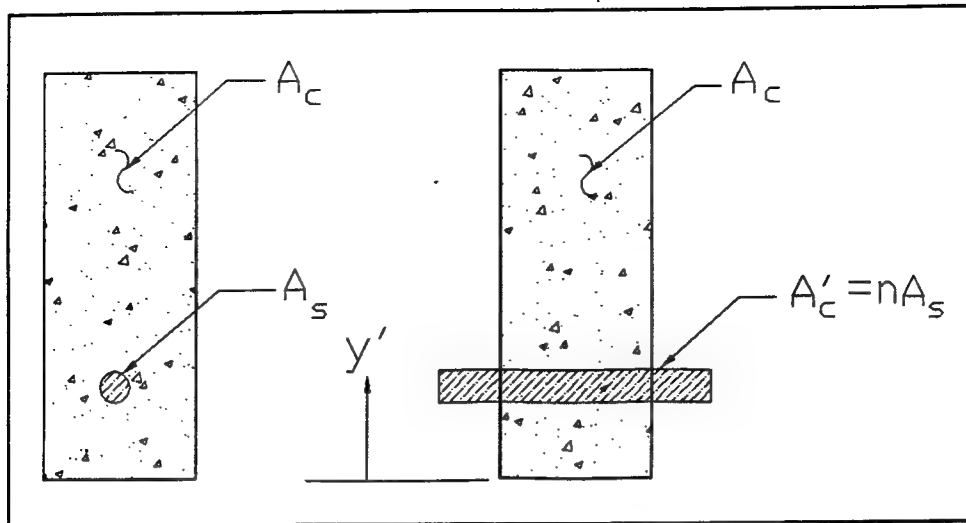


Figure 8. Graphic representation of a transformed section where  $y'$  is the centroid of the transformed section

$n$  = ratio of steel modulus to concrete modulus

$\sigma_c$  = stress in concrete

Now that all the equations necessary for computing stresses to compare to the finite element solutions have been presented, problems with numerical values can be performed.

## Example Problems

As in Chapter 2, examples for a beam in bending will be presented to show how solutions can be obtained through hand calculations and how these results compare to the solutions obtained numerically from ABAQUS.

### Unreinforced beam

A simply supported beam is shown in Figure 9. For discussions presented in this section it will be assumed that the beam does not contain any reinforcing. Dimensions of the beam and the applied load are provided in the figure. The arrangement of this beam is identical to the beam shown in Figure 6 from which the equations for stress were developed. Therefore, the equations developed from Figure 6 will apply to calculations done for the beam shown in Figure 9. It should also be noted that the width shown in Figure 9 is for a strip of unit width.

The moment in the center of the beam due to the applied loading must first be calculated using Equation 21,

$$M = \frac{pa^2}{2} = \frac{(12 \text{ lb./in.})(42 \text{ in.})^2}{2}$$

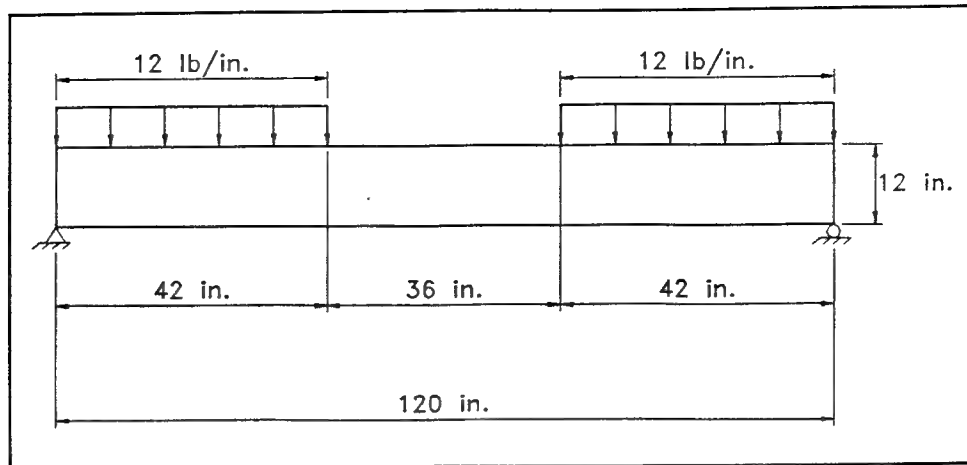


Figure 9. Simply supported beam geometry and loading

$$M = 10,584 \text{ in.-lb.}$$

The moment of inertia must also be calculated and is given by

$$I = \frac{bh^3}{12} = \frac{(1 \text{ in.})(12 \text{ in.})^3}{12}$$

$$I = 144 \text{ in.}^4$$

where

$b$  = width of the member cross section

$h$  = height of the member cross section

This moment may then be used to compute the stress at the extreme fiber of the beam, so for tension at the bottom of the beam, the stress as computed by Equation 22 is

$$\sigma = \frac{My}{I} = \frac{-(10,584 \text{ lb.-in.})(-6 \text{ in.})}{144 \text{ in.}^4}$$

$$\sigma = 441.0 \text{ psi}$$

Since the default for ABAQUS stress output is at the integration points and not at the nodes, the location of the integration points must be determined and used in the hand solution for a valid comparison with numerical results. The finite element mesh used to model the beam is shown in Figure 10. Eight noded, reduced integration, plane stress elements are used to perform the analysis. A reduced integration element has four integration points which will be located at distance of 0.2113 times the total element length from the edge of the element. Therefore, for the 6-in. elements used, the integration points will be located 1.268 in. from the edges of the elements and the distance  $y$  used in Equation 22



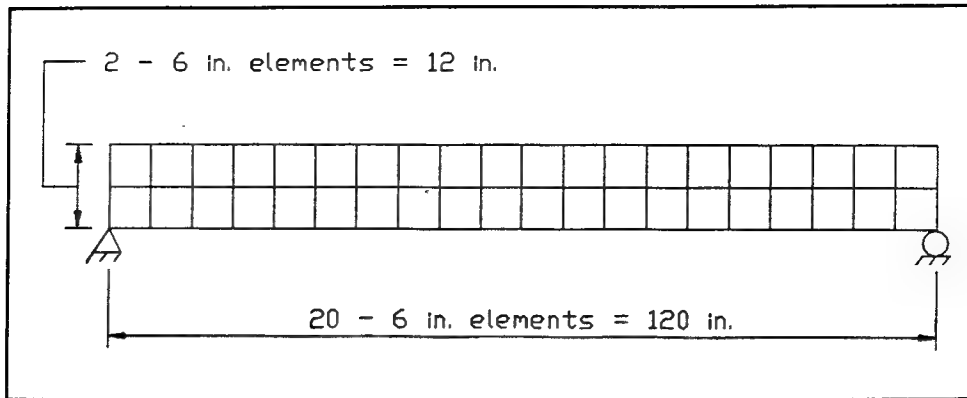


Figure 10. Finite element mesh for simply supported beam

will be 4.732 in. (6.0 in. - 1.268 in.). The stress at the integration point nearest the bottom of the beam will be

$$\sigma = \frac{-(10,584 \text{ lb.-in.})(-4.732 \text{ in.})}{144 \text{ in.}^4} = 347.81 \text{ psi}$$

This matches exactly with the stress calculated by ABAQUS of 347.8 psi.

### Reinforced beam

The beam shown in Figure 9 will be used again for demonstrating calculations for a reinforced beam. It will be assumed that unit strip shown in Figure 9 is taken from a beam 12 in. in width and that the beam contains a single #9 reinforcing bar with the center of the bar located 3 in. from the bottom of the beam. Since the beam is 12 in. wide, the area of steel per unit width is  $0.0833 \text{ in.}^2$ . The reinforcing steel has a modulus of 29,000,000 psi, while the concrete has a modulus of 4,045,000 psi. Therefore, the ratio of the steel modulus to the concrete modulus is

$$n = \frac{E_s}{E_c} = \frac{29,000,000 \text{ psi}}{4,045,000 \text{ psi}}$$

$$n = 7.17$$

This value of  $n$  can now be used to transform the area of steel into an equivalent area of concrete  $A_c'$ .

$$A_c' = nA_s = 7.17(0.0833) = 0.5975 \text{ in.}^2$$

Since the area of the concrete has changed due to the transformed section, the centroid and moment of inertia of the transformed section must be calculated before the stress in the beam can be computed. The transformed centroid  $y'$  from the bottom of the beam is

$$y' = \frac{(1 \text{ in.})(12 \text{ in.})(6 \text{ in.}) + (0.5975 \text{ in.}^2)(3 \text{ in.})}{(1 \text{ in.})(12 \text{ in.}) + (0.5975 \text{ in.}^2)}$$

$$y' = 5.858 \text{ in.}$$

The moment of inertia can also be calculated using the following equation,

$$I = (bh^3)/12 + A_C d_C^2 + (n - 1)A_S d_S^2$$

where

$b$  = width of beam (1 in.)

$h$  = depth of beam (12 in.)

$A_C$  = area of concrete

$d_C$  = distance from centroid of section to centroid of concrete

$A_S$  = area of steel

$d_S$  = distance from centroid of section to centroid of steel

Substituting the appropriate values, the moment of inertia for the beam is

$$I = \frac{(1 \text{ in.})(12 \text{ in.})^3}{12} + (1 \text{ in.})(12 \text{ in.})(6 \text{ in.} - 5.858 \text{ in.})^2$$

$$+ (0.5975 \text{ in.}^2)(5.858 \text{ in.} - 3 \text{ in.})^2$$

$$I = 149.12 \text{ in.}^4$$

The maximum tensile stress at the base of the beam can also be calculated using Equation 22. The moment will be the same as was calculated previously for the unreinforced beam since the moment is only dependent on the loading and the geometry of the beam. Therefore, the maximum tensile stress is

$$\sigma_c = \frac{-(10,584 \text{ lb.-in.})(-5.858 \text{ in.})}{149.12 \text{ in.}^4} = 415.8 \text{ psi}$$

The maximum tensile stress for the unreinforced beam was 441.0 psi. For an uncracked section it can be seen that adding reinforcing in a beam does provide some reduction in stress to the concrete, but that this reduction is minimal. The primary benefit of including reinforcing in concrete is that after cracking the reinforcement will carry the load which had previously been carried by the concrete. This will be demonstrated later in this chapter as well as in Chapters 4 and 5.

As for the unreinforced problem, the stress in the beam must be calculated at the same location as an integration point in order to obtain a direct comparison of the concrete stress. The distance from centroid of the section to integration point was computed previously to be 4.732 in. This distance must be modified since the centroid of the transformed section has changed. The new value is

$$y = -4.732 \text{ in.} + (6.0 \text{ in.} - 5.858 \text{ in.}) = -4.590 \text{ in.}$$

So, the stress at the location of the integration point is

$$\sigma_c = \frac{-(10,584 \text{ in.-lb.})(-4.590 \text{ in.})}{149.12 \text{ in.}^4} = 325.8 \text{ psi}$$

Results of the numerical analysis using ABAQUS gives a stress of 325.8 psi, matching exactly the hand calculation. In addition, an analysis was performed using the UMAT subroutine which includes the aging characteristics of the concrete. For comparison purposes, the effects of creep and shrinkage were removed. Since the UMAT subroutine is contained in the ANACAP-U software (ANATECH Research Corp. 1992), the removal of creep and shrinkage was done numerically and not by altering the UMAT subroutine. The maximum stress from this analysis was 325.6 psi, which is almost identical to the hand calculation and the elastic analysis using ABAQUS.

To obtain the stress in the steel, the stress in the concrete at the location of the steel in the beam must first be computed. The reinforcing is centered 3 in. above the bottom of the beam, so the distance from the centroid of the section to the location of the steel  $y_s$  is

$$y_s = -(5.858 \text{ in.} - 3.0 \text{ in.}) = -2.858 \text{ in.}$$

Using this value of  $y_s$  in Equation 22 gives

$$\sigma_c = \frac{-(10,584 \text{ lb.-in.})(-2.858 \text{ in.})}{149.12 \text{ in.}^4} = 202.8 \text{ psi}$$

The stress in the steel can be calculated by simply multiplying the above computed concrete stress by the previously calculated ratio of steel modulus to concrete modulus.

$$\sigma_s = n\sigma_c = 7.170(202.8 \text{ psi})$$

$$\sigma_s = 1454.3 \text{ psi}$$

As with the preceding calculations, the results between the hand computations and ABAQUS output from the elastic case match exactly. The stress output by ABAQUS for the reinforcing was 1,454 psi using purely elastic parameters. The stress reported by ABAQUS for the case using the aging modulus was 1,469 psi, which is still within 1 percent of the other computed values.

Finally, an analysis was performed with an increased load which will cause a crack to form in the beam. The distributed load on each end of the beam was increased to 15.0 lb./in. This load was sufficient to increase the stresses in the concrete to the point where cracking will occur in the ABAQUS analysis. The results from ABAQUS analysis will then be compared to hand calculations which take into account the fact that a portion of the concrete beam is cracked.

To improve the comparison, the model used to perform the analysis was revised from a mesh of 2 by 20 to 4 by 40. Since cracking in the analysis causes

the problem to become nonlinear, increasing the density of the mesh will be beneficial in increasing the accuracy of the finite element solution.

In order to calculate the stresses in the concrete and reinforcing for the case where the beam has cracked, the value of tensile strain at which cracking occurs must be assumed. For the loading used in this problem, the uniaxial strain at cracking of 0.0001 in./in. may be used. Based on this assumption, the equilibrium diagram may be established as shown in Figure 11. Based on the diagram, equilibrium is satisfied by summing the moments about the neutral axis which gives

$$\left(\frac{2c}{3}\right)C_c - \left(\frac{2c'}{3}\right)T_c - (9 - c)T_s - M = 0 \quad (24)$$

where

- $c$  = distance from extreme compression fiber to the neutral axis
- $C_c$  = compression force in the concrete
- $T_c$  = tension force in the concrete
- $T_s$  = tension force in the reinforcing steel
- $M$  = moment applied to the beam (13,230 in.-lb.)

Each of the above forces can be computed as follows:

$$C_c = \frac{1}{2}f_c c b = \frac{1}{2}\epsilon_c E_c c b \quad (25)$$

$$T_c = \frac{1}{2}f_t c' b = \frac{1}{2}(0.0001)E_c c' b \quad (26)$$

$$T_s = E_s A_s \epsilon_s \quad (27)$$

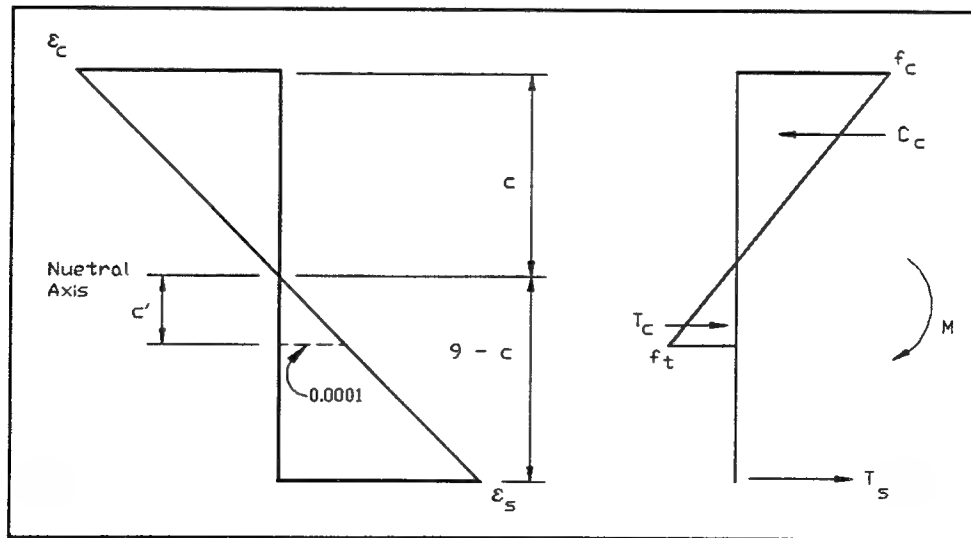


Figure 11. Stress distribution through depth of beam for cracked and uncracked sections

where

$f_c$  = compressive stress at extreme fiber

$E_c$  = compressive strain at extreme fiber

$f_t$  = tensile stress capacity

$c'$  = distance from neutral axis to stress equivalent to tensile stress capacity

$E_s$  = strain in reinforcing steel

Using the diagrams in Figure 11 and similar triangles, the following two equations may be derived:

$$c' = 0.0001 \left( \frac{c}{\epsilon_c} \right) \quad (28)$$

$$\epsilon_s = \epsilon_c \left( \frac{9 - c}{c} \right) \quad (29)$$

Inserting Equations 28 and 29 into Equations 26 and 27 and then substituting Equations 25-27 into Equation 24, the resulting equation is

$$\left( \frac{\epsilon_c E_c}{3} \right) c^2 - \left[ \frac{(0.0001) E_c}{3} \right] \left[ \frac{(0.0001) c}{\epsilon_c} \right]^2 - \left( \frac{E_s A_s \epsilon_c}{c} \right) (9 - c)^2 - M = 0$$

Multiplying this equation by  $c$  and regrouping terms results in

$$\left[ \frac{\epsilon_c E_c}{3} + \frac{(1 \times 10^{-12}) E_c}{3 \epsilon_c} \right] c^3 + (E_s A_s \epsilon_c) c^2 - (18 E_s A_s \epsilon_c + M) c + 81 E_s A_s \epsilon_c = 0 \quad (30)$$

Both  $c$  and  $\epsilon_c$  are unknowns and therefore the equation must be solved iteratively. Performing the iterative calculations results in a value of 2.864 in. for the value of  $c$  and 0.0003063 for  $\epsilon_c$ .

It is known that the stress in the reinforcing can be computed by

$$\sigma_s = E_s \epsilon_s$$

Substituting for  $\epsilon_s$  using Equation 29 will give

$$\sigma_s = E_s \epsilon_c \left( \frac{9 - c}{c} \right) \quad (31)$$

Likewise, the stress at the extreme fiber of the concrete at the top of the beam may be computed by

$$\sigma_c = E_c \epsilon_c \quad (32)$$

Stresses at any location in the uncracked portion of the beam may be obtained by linear interpolation once the extreme fiber stress is known by using simple linear interpolation.

Using the values for  $c$  and  $\epsilon_c$  computed from Equation 30, the stress in the reinforcing can be computed using Equation 31:

$$\sigma_s = (29.0 \times 10^6 \text{ psi})(0.0003063 \text{ in./in.}) \left( \frac{9 \text{ in.} - 2.864 \text{ in.}}{2.864 \text{ in.}} \right)$$

$$\sigma_s = 19,026 \text{ psi}$$

This can be compared to 18,272 psi stress in the reinforcing as calculated by ABAQUS. This is less than a 4 percent difference between the two methods, which is excellent agreement for comparison to a nonlinear type problem. As mentioned previously, adjustments to eliminate creep and shrinkage had to be accounted for numerically, which is not an exact method for eliminating these effects; therefore, some of the difference may be attributed to the adjustment to the creep and shrinkage.

Using Equation 32 now to compute the stress at the extreme fiber of the concrete:

$$\sigma_c = (4.045 \times 10^6 \text{ psi})(0.0003063 \text{ in./in.}) = 1,239 \text{ psi}$$

Since output of stresses at the nodes was not requested, a stress must be calculated at the location of an element integration point as has been done in the past. Since the elements are 3 in. high, then the first integration point from the top of the beam will be located 0.634 in. down. It is known that the stress in the concrete is zero at the neutral axis, which is 2.864 in. from the top of the beam. The stress at 0.634 in. from the top of the beam can be calculated using a ratio of these distances times the extreme fiber concrete stress as follows:

$$\sigma'_c = (1,239 \text{ psi}) \left( \frac{2.864 \text{ in.} - 0.634 \text{ in.}}{2.864 \text{ in.}} \right) = 965 \text{ psi}$$

This can be compared to the ABAQUS result of 1,010 psi which is approximately 4.5 percent higher than the hand solution and some of the difference may once again be attributed to the fact that the effect of creep and shrinkage could not entirely be eliminated from the model.

## Summary

As has been described, agreement between hand calculations and ABAQUS results were exact for the cases where the ABAQUS solutions were based on a linear elastic assumption, and for cases where the UMAT model was used the comparisons were still very good. Even for the highly nonlinear case where cracking occurred, hand calculations provided respectable agreement with the

numerical results. These calculations further demonstrate how the use of reinforcing will provide reliable results.

## 4 Analyses of a Slab

---

### Introduction

The final example to be demonstrated will be of a slab containing two lifts of concrete. This example was chosen so that incremental construction could be demonstrated. The slab will be fully supported along its base and will be subjected to a uniform temperature gradient through the depth with the coldest temperature at the top of the slab. This loading will create a tension condition at the top of the slab. This type of loading is similar to the loading which occurs in the base slab of a u-frame lock monolith supported on piles. As with the previous examples, the general formulation for calculating stresses will be presented followed by using actual values to illustrate how the equations are applied.

### Problem Formulation

#### Unreinforced problem

The initial set of computations performed on the slab will assume that the two lifts are made of the same material. This in essence eliminates the lift construction, but evaluating the problem as a single material will be beneficial in the development of equations.

As described in Chapter 2, the stress observed in a structure is a function of both the changes in temperature which occur and the structure's restraining boundary conditions. Essentially, thermal stresses result from restrained displacements, i.e., displacements that would normally occur due to induced temperature changes if restraining boundary conditions were not present. In the case of the slab, as shown in Figure 12a, a temperature gradient with cold temperatures at the top of the slab and hot temperatures at the base causes the slab to want to bend and deflect as shown in Figure 12b, but due to the support conditions it is being prevented from doing so. Since the deflection that is being restrained is a bending mechanism, then the resulting strain state will be a linear strain distribution from the bottom of the slab to the top of the slab as shown in Figure 12c. Since the change in temperature is linear and the material is uniform, the strain at any given height in the slab can be found by determining the temperature change using linear interpolation and applying the following equation:



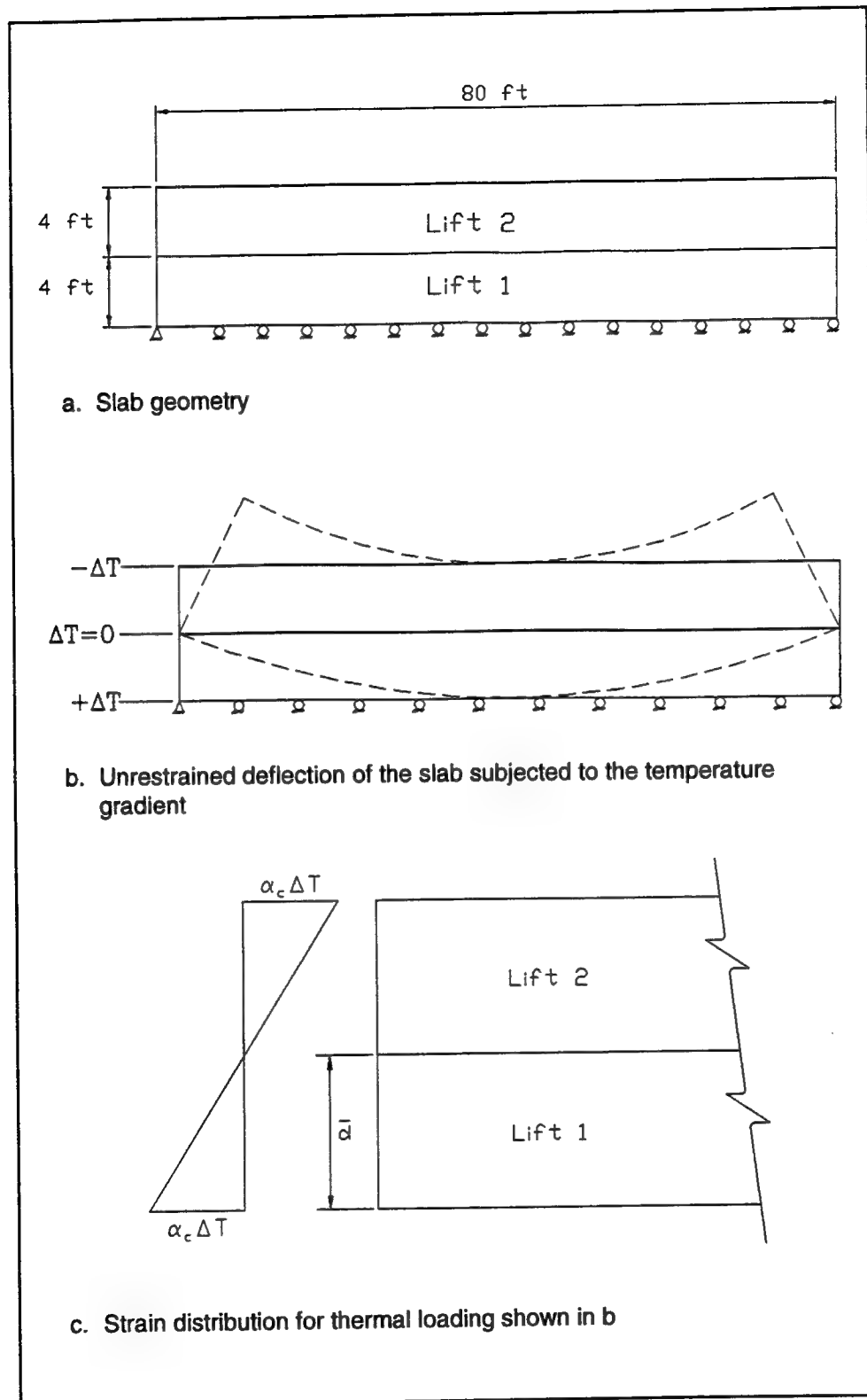


Figure 12. Two-lift slab

$$\epsilon = \alpha_c \Delta T \quad (33)$$

where

$\epsilon$  = strain in concrete

$\alpha_c$  = coefficient of thermal expansion of the concrete

$\Delta T$  = change in temperature

The strain computed may then be used to compute the associated stress by:

$$\sigma_c = E_c \epsilon \quad (34)$$

where

$\sigma_c$  = stress in concrete

$E_c$  = modulus of elasticity of the concrete

If the problem is evaluated using two different materials corresponding to the two lifts, then Equations 33 and 34 still apply, but the hand calculations must be revised based on a transformed section. The method for obtaining a transformed section is the same as was described in Chapter 3, but instead of transforming a steel bar to an equivalent modulus of the concrete, one lift of concrete will need to be transformed to be equivalent to the modulus of the other lift. This will require the neutral axis to be computed for the transformed section.

As in Chapter 3, the ratio of the moduli of elasticity for two different materials is used for computing equivalent transformed sections. This ratio  $n$  is given by:

$$n = \frac{E_{c2}}{E_{c1}} \quad (35)$$

where

$E_{c1}$  = modulus of elasticity for concrete lift 1

$E_{c2}$  = modulus of elasticity for concrete lift 2

This ratio can then be used in the computation of the neutral axis as follows:

$$\bar{d} = \frac{A_1 y_1 + n A_2 y_2}{A_1 + n A_2} \quad (36)$$

where

$\bar{d}$  = distance from base to neutral axis of the transformed section

$A_1$  = cross-sectional area of lift 1

$y_1$  = distance from base to centroidal axis of lift 1

$A_2$  = cross-sectional area of lift 2

$y_2$  = distance from base to centroidal axis of lift 2

The resulting strain due to the temperature gradient will be as shown in Figure 13, where zero strain is located at the neutral axis. The total strain can be defined as shown in Figure 13 by a linearly varying strain component and a uniform strain component. The strain as shown in Figure 13 can be defined in equation form by

$$\epsilon = \epsilon_{LV} + \epsilon_{NA} \quad (37)$$

where

$\epsilon$  = total strain in the concrete at a specified height

$\epsilon_{LV}$  = linearly varying strain component at a specified height, symmetrical about midheight of the slab

$\epsilon_{NA}$  = uniform strain component

$\epsilon_{LV}$  may be computed using Equation 33 to compute the strain at the extreme fiber and then using similar triangles to compute the strain at the desired location.  $\epsilon_{NA}$  can be computed using the following equation

$$\epsilon_{NA} = \frac{\left( \frac{h}{2} - \bar{d} \right) (\alpha_c \Delta T)}{\frac{h}{2}} \quad (38)$$

where  $h$  = height of the slab. Once the total strain has been computed using Equation 37, then the stress at the specified height may also be computed using Equation 34.

### Reinforced problem

Performing the calculations for a reinforced slab will be nearly identical to the calculations performed for the slab with two lifts of two different moduli outlined above except there will be an additional ratio  $n_s$  which will be the ratio

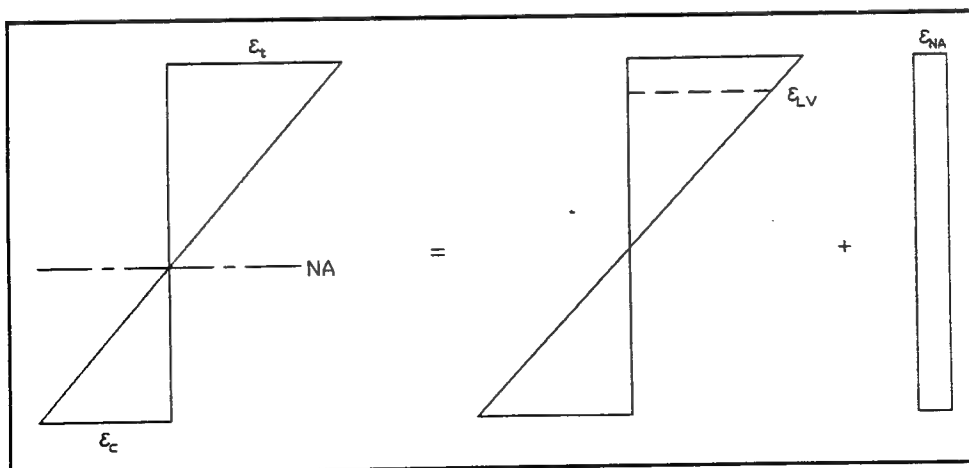


Figure 13. Strain distribution for a thermal loading of a two-lift slab

of the steel modulus to the modulus of lift 1. Therefore, the transformed section will be a section which consists of the modulus from lift 1 with areas for lift 2 and the reinforcing adjusted accordingly. The ratio  $n_s$  is given by

$$n_s = \frac{E_s}{E_{cl}}$$

where  $E_s$  = modulus of reinforcing steel. A similar calculation to Equation 36 may then be performed to obtain the neutral axis of the transformed section as follows

$$\bar{d} = \frac{A_1 y_1 + n A_2 y_2 + n_s A_{ST} y_{ST} + n_s A_{SB} y_{SB}}{A_1 + n A_2 + n_s A_{ST} + n_s A_{SB}} \quad (39)$$

where

$A_{ST}$  = area of reinforcing in the top of slab

$y_{ST}$  = distance from base to center of reinforcing in the top of slab

$A_{SB}$  = area of reinforcing in the bottom of slab

$y_{SB}$  = distance from base to center of reinforcing in the bottom of slab

Once the neutral axis has been established, then the equations used previously for the two unreinforced lifts with different moduli can be used to compute the stress and strain in the concrete. Equation 34 can be used to compute the stress in the concrete, but the stress in the reinforcing must be computed by

$$\sigma_s = E_s \epsilon \quad (40)$$

## Example Problems

As in Chapters 2 and 3, examples for a slab with a temperature gradient applied through its thickness are presented to show how solutions can be obtained through hand calculations and how these results compare to the solutions obtained numerically from ABAQUS.

### Unreinforced slab

The dimensions of the slab to be evaluated are shown in Figure 12a. The finite element mesh used to analyze the slab is shown in Figure 14. The first analysis was performed using the same modulus of elasticity ( $4.042 \times 10^6$  psi) for both lifts. The gradient applied was 24 °F through the thickness of the slab, with a temperature at the base of 46 °F and a temperature at the top of 70 °F. The initial temperature prior to application of the gradient was 58 °F and was uniform through the slab thickness. The coefficient of thermal expansion of the concrete is  $4.0 \times 10^{-6}$  in./in./°F. Using Equation 33, the strain at the top of the slab is given by

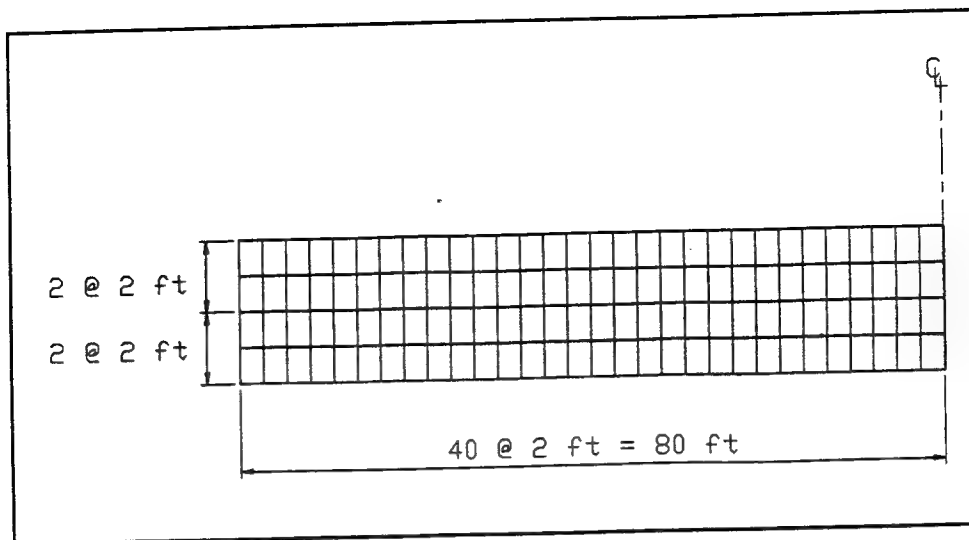


Figure 14. Finite element mesh of slab

$$\epsilon = (4.0 \times 10^{-6} \text{ in./in./}^{\circ}\text{F})(12^{\circ}\text{F})$$

$$\epsilon = 48.0 \times 10^{-6} \text{ in./in.}$$

Since comparison to the numerical results is desired, the strain at the location of the integration points must be computed. As an example, perform the calculation at the top integration point of the slab which is located 90.928 in. from the bottom of the base. Since the temperature varies linearly (as does the strain), the strain calculation can be done using Equation 33 and by interpolating to the point desired since the neutral axis is intuitively known to be located 48 in. from the base.

$$\epsilon = \frac{90.928 \text{ in.} - 48.0 \text{ in.}}{48 \text{ in.}} (12^{\circ}\text{F}) (4.0 \times 10^{-6} \text{ in./in./}^{\circ}\text{F})$$

$$\epsilon = 42.93 \times 10^{-6} \text{ in./in.}$$

Now, knowing the strain at the location of the integration point, the stress at this location may be computed using Equation 34.

$$\sigma_c = (4.042 \times 10^6 \text{ psi})(42.93 \times 10^{-6} \text{ in./in.})$$

$$\sigma_c = 173.5 \text{ psi}$$

This result matches exactly with the results from ABAQUS. Table 5 shows resulting stresses from hand calculations and ABAQUS results at all of the integration points through the slab thickness. As can be seen in the table the two sets of results compare exactly.

**Table 5**  
**Stresses in Slab (Same Material in Both Lifts)**

Distance from Base to Integration Point, in.	Resulting Stresses, psi	
	Hand Calculation	ABAQUS
90.9282	173.5	173.5
77.0718	117.5	117.5
66.9282	76.5	76.5
53.0718	20.5	20.5
42.9282	-20.5	-20.5
29.0718	-76.5	-76.5
18.9282	-117.5	-117.5
5.0718	-173.5	-173.5

Using the same geometry and the same finite element mesh, the calculations will be performed using different modulus of elasticity values for the two lifts. The values of modulus for each lift will be:

$$\text{Lift 1} - E_{C1} = 4.042 \times 10^6 \text{ psi}$$

$$\text{Lift 2} - E_{C2} = 3.684 \times 10^6 \text{ psi}$$

So if the calculations are performed using the modulus of lift 1, then the ratio of modulus  $n$  can be computed using Equation 35 and results in

$$n = \frac{E_{C2}}{E_{C1}} = \frac{3.684 \times 10^6 \text{ psi}}{4.042 \times 10^6 \text{ psi}} = 0.9114$$

Lift 2 must be transformed into an equivalent section for a modulus of  $E_1$  and therefore the neutral axis will no longer be at the midheight of the slab. The neutral axis of the transformed section may be computed using Equation 36 as follows

$$\bar{d} = \frac{(0.9114 \text{ in.})(48 \text{ in.})(72 \text{ in.}) + (1 \text{ in.})(48 \text{ in.})(24 \text{ in.})}{(0.9114 \text{ in.})(48 \text{ in.}) + (1 \text{ in.})(48 \text{ in.})}$$

$$\bar{d} = 46.888 \text{ in.}$$

To compute the strain for this case, Equation 37 may be used. For the top of the slab, the linearly varying strain component  $\epsilon_{LV}$  will be identical to strain computed previously for the case of uniform material. The uniform strain component  $\epsilon_{NA}$  can be computed using Equation 38 as follows

$$\epsilon_{NA} = \frac{\left( \frac{96 \text{ in.}}{2} - 46.888 \text{ in.} \right) (4.0 \times 10^{-6} \text{ in./in./}^{\circ}\text{F})(12 \text{ }^{\circ}\text{F})}{\frac{96 \text{ in.}}{2}}$$

$$\epsilon_{NA} = 1.11 \times 10^{-6} \text{ in./in.}$$

Therefore, using Equation 37, the total strain will be

$$\epsilon = 48.0 \times 10^{-6} \text{ in./in.} + 1.11 \times 10^{-6} \text{ in./in.}$$

$$\epsilon = 49.11 \times 10^{-6} \text{ in./in.}$$

As for the previous case, the calculations must be performed at the integration points to be able to compare to the ABAQUS results. The calculation for the top integration point in the slab will be presented. The strain computed previously for the uniform slab will be the component for the linearly varying strain  $\epsilon_{LV}$ . Since the uniform strain component is constant throughout the height of the slab, it will be the same as was computed above; the total strain will be

$$\epsilon = 42.93 \times 10^{-6} \text{ in./in.} + 1.11 \times 10^{-6} \text{ in./in.}$$

$$\epsilon = 44.04 \times 10^{-6} \text{ in./in.}$$

Now, compute the stress using Equation 34 but use the modulus of elasticity for lift 2 since the integration point is located in lift 2

$$\sigma_c = (3.684 \times 10^6 \text{ psi})(44.04 \times 10^{-6} \text{ in./in.})$$

$$\sigma_c = 162.2 \text{ psi}$$

This value matches the ABAQUS result exactly. Results of hand calculations and numerical results are shown in Table 6. The ABAQUS analysis was performed both with and without the user material subroutine, UMAT. As can be seen in the table, the ABAQUS results which do not include the UMAT subroutine match exactly with the hand calculations. Some variation does exist when comparing to the ABAQUS results using the UMAT subroutine. As discussed in Chapter 3, removal of creep and shrinkage was done numerically, which is not an exact method of removal; and, therefore, some creep and shrinkage may still be included.

### Reinforced slab

The example for the reinforced slab will be identical to the unreinforced slab except that the slab will include reinforcing in both the top and the bottom of the slab. The size of the reinforcement used was #18 bars, spaced at 12 in. in the out-of-plane direction. Assuming that 4 in. of clear cover exists at both the top and the bottom of the slab, the center of the reinforcing was located 5.125 in. from the horizontal surfaces of the slab.

**Table 6**  
**Stresses in Slab (Different Materials in Lifts)**

Distance from Base to Integration Point, in.	Resulting Stresses, psi		
	Hand Calculation	ABAQUS w/o UMAT	ABAQUS with UMAT
90.9282	162.2	162.2	162.9
77.0718	111.2	111.2	111.6
66.9282	73.8	73.8	74.0
53.0718	22.8	22.8	22.7
42.9282	-16.0	-16.0	-16.3
29.0718	-72.0	-72.0	-72.3
18.9282	-113.0	-113.0	-113.3
5.0718	-169.0	-169.0	-169.3

The coefficient of thermal expansion values are the same as used in Chapter 2. The modulus of elasticity values for lifts 1 and 2 will be the same as those used for the unreinforced slab and the modulus for the steel will be 29,000,000 psi. The ratio of lift 2 modulus to lift 1 modulus  $n$  will again be 0.9114, and the ratio of steel modulus to the lift 1 modulus will be:

$$n_s = \frac{E_s}{E_{Cl}} = \frac{29.0 \times 10^6 \text{ psi}}{4.042 \times 10^6 \text{ psi}} = 7.175$$

Since the reinforcing has been added, the neutral axis will need to be computed again based on Equation 39 and the areas of the transformed sections as shown in Figure 15. Substituting the appropriate values into Equation 39 results in

$$\bar{d} = 46.943 \text{ in.}$$

As for the unreinforced case, the strain may now be computed using Equation 37. If the strain at the top of the slab is being computed, then  $\epsilon_{LV}$  will be  $48.0 \times 10^{-6}$  in./in. as previously computed, and the uniform strain component can be computed using Equation 38.

$$\epsilon_{NA} = \frac{\left( \frac{96 \text{ in.}}{2} - 46.943 \text{ in.} \right) (4.0 \times 10^{-6} \text{ in./in./}^\circ\text{F})(12 \text{ }^\circ\text{F})}{\frac{96 \text{ in.}}{2}}$$

$$\epsilon_{NA} = 1.057 \times 10^{-6} \text{ in./in.}$$



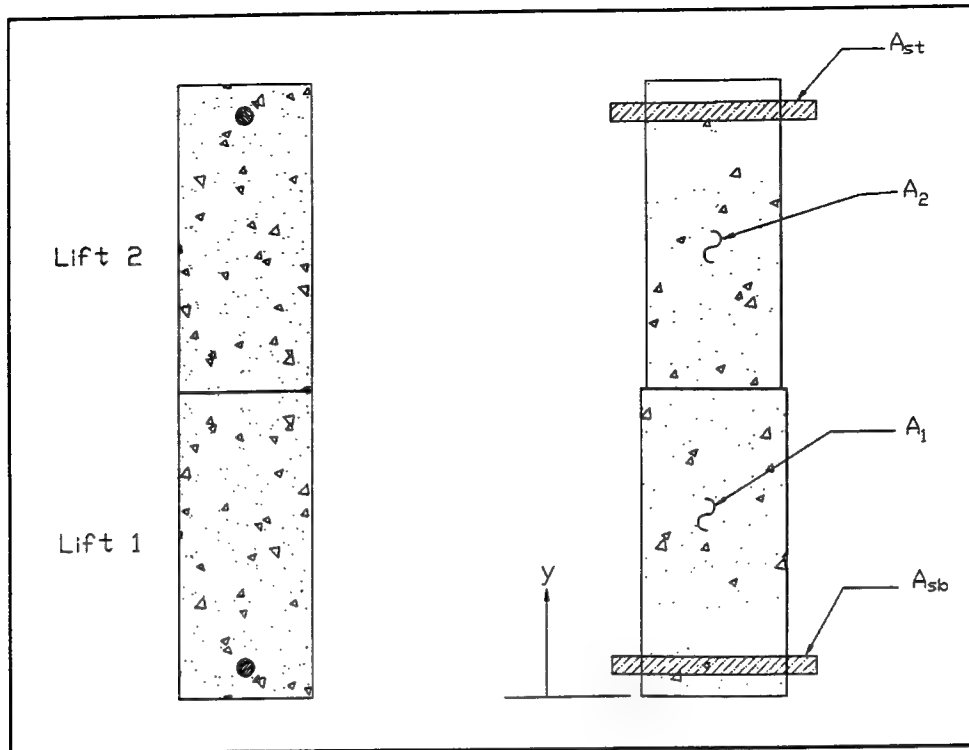


Figure 15. Transformed section of reinforced slab

Using Equation 37 gives the total strain

$$\epsilon = 48.0 \times 10^{-6} \text{ in./in.} + 1.06 \times 10^{-6} \text{ in./in.}$$

$$\epsilon = 49.06 \times 10^{-6} \text{ in./in.}$$

These calculations must now be repeated at the integration points. For the integration point near the top of the slab, the value of  $42.93 \times 10^{-6} \text{ in./in.}$  may be used for  $\epsilon_{LV}$  and  $1.06 \times 10^{-6} \text{ in./in.}$  may be used for  $\epsilon_{NA}$ . So, using Equation 37 results in:

$$\epsilon = 42.93 \times 10^{-6} \text{ in./in.} + 1.06 \times 10^{-6} \text{ in./in.}$$

$$\epsilon = 43.99 \times 10^{-6} \text{ in./in.}$$

As before, the stress in the concrete can be found using Equation 34:

$$\sigma_c = (3.684 \times 10^6 \text{ psi})(43.99 \times 10^{-6} \text{ in./in.})$$

$$\sigma_c = 162.1 \text{ psi}$$

Similar calculations can be done at other integration points and result in the values shown in Table 7. Some very small differences occur at the top and bottom of the slab for the ABAQUS results without the UMAT subroutine, but

in general the results match exactly. As before, the values for the ABAQUS analysis which used UMAT varied slightly from the hand calculations.

<b>Table 7 Stresses in Slab with Reinforcing (Different Materials in Lifts)</b>			
Distance from Base to Integration Point, in.	Resulting Stresses, psi		
	Hand Calculation	ABAQUS w/o UMAT	ABAQUS with UMAT
90.9282	162.0	162.1	162.8
77.0718	111.0	111.0	111.4
66.9282	73.6	73.6	73.8
53.0718	22.6	22.6	22.5
42.9282	-16.2	-16.2	-16.5
29.0718	-72.2	-72.2	-72.5
18.9282	-113.2	-113.2	-113.5
5.0718	-169.2	-169.3	-169.6
90.875 (top reinf.)	2051.2	2051.	2049.
5.125 (btm. reinf.)	-1989.9	-1990.	-1992.

The stresses in the steel reinforcing may also be computed and compared to the numerical results. The total strain must be calculated at the elevations of the reinforcing bars. Taking the top bar as an example, the linearly varying strain is calculated as before except the coefficient of thermal expansion of the steel  $\alpha_s$  must be used instead of  $\alpha_c$ :

$$\epsilon_{LV} = \frac{90.875 \text{ in.} - 48.0 \text{ in.}}{48 \text{ in.}} (12 \text{ }^\circ\text{F}) (6.5 \times 10^{-6} \text{ in./in./}^\circ\text{F})$$

$$\epsilon_{LV} = 69.67 \times 10^{-6} \text{ in./in.}$$

So the total strain at the elevation of the top reinforcing bar will be:

$$\epsilon = 69.67 \times 10^{-6} \text{ in./in.} + 1.06 \times 10^{-6} \text{ in./in.}$$

$$\epsilon = 70.73 \times 10^{-6} \text{ in./in.}$$

The stress in the reinforcement can now be found using Equation 40:

$$\sigma_s = (29 \times 10^6 \text{ psi}) (70.73 \times 10^{-6} \text{ in./in.})$$

$$\sigma_s = 2051.2 \text{ psi}$$

This compares very well with the ABAQUS results as do the results for the reinforcement located at the bottom of the slab.

## Summary

As in the previous two chapters, comparisons between analytical and numerical solutions were very good. The slab problem presented in this chapter demonstrates that even for complicated conditions, the resulting stresses can be predicted and verified. Being able to predict the stresses in an incremental construction problem such as the problem analyzed in this chapter should provide the confidence in the numerical methods used when reinforcing is included in an analysis of a full-scale massive concrete structure.

## 5 Analyses of a Lock Chamber Monolith

---

### Introduction

Chapters 2, 3, and 4 provided valuable insight into how stresses in reinforcing can be calculated and then compared to numerical solutions for some simple, straightforward problems. These problems were presented to gain an understanding of the mechanics involved in doing these computations and to provide confidence that the analysis tools will provide reliable results. In order to expand that understanding, analyses of a full-scale massive concrete structure should be evaluated with reinforcing included and with cracking occurring.

Results of analyses performed on a typical chamber monolith for the Olmsted Locks will be presented to show the effects of reinforcing for an uncracked condition and for a case when cracking does occur. Results of the analyses presented herein are further documented in Merrill, Fehl, and Garner (1995). The first set of results presented will compare the results of an analysis of the monolith with no reinforcing to an analysis of the monolith including reinforcing according to the reinforcing layout shown in Figure 16. The second set of results will present results of an analysis which exhibited no cracking compared to an analysis with cracking.

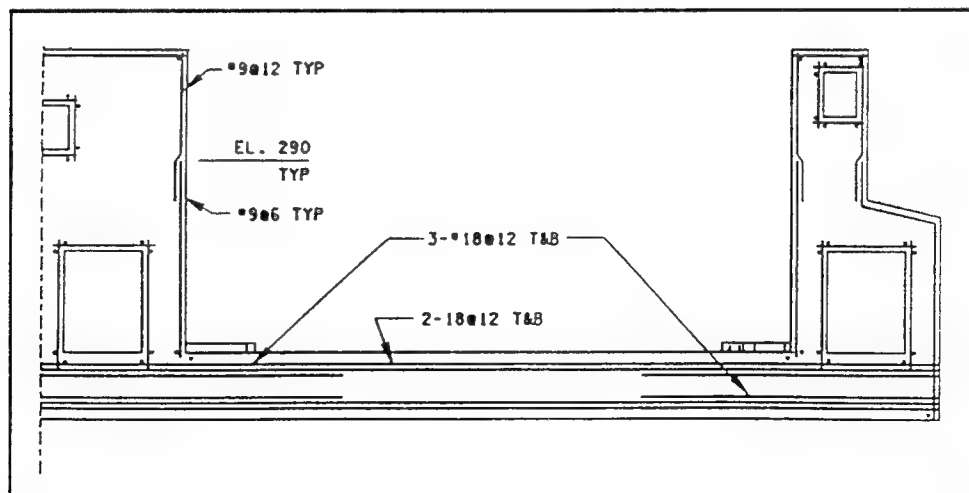


Figure 16. Reinforcing layout for chamber monolith at Olmsted Locks

## No Reinforcing Versus Reinforcing

Early NISA studies (Melvin Price Locks and Dam and Red River Locks and Dam) did not account for the reinforcing in the structures. In addition, most of the analyses performed for the NISA study of the typical chamber monolith for the Olmsted Locks did not include reinforcing. It was during the course of the Olmsted study that inclusion of reinforcing in the model became necessary. As a prelude to including reinforcing into these two monoliths, reinforcing was added to the typical chamber monolith finite element model and the analysis was performed again.

The plots shown in Figures 17-21 are comparisons between the analysis with no reinforcing included and the analysis with reinforcing incorporated. Figures 17-19 are comparisons of the horizontal stress at points within the slab of the monolith. As can be seen in the figures, inclusion of reinforcing does reduce the maximum stress for each of the three points shown. This is due to the fact that the change in ambient temperature creates a bending-type mechanism in the slab as described in Chapter 4, and since the reinforcing increases the moment of inertia of the slab, the result of adding reinforcing is a slight decrease in the stress.

Figures 20 and 21 are plots of the maximum principal stress at points in the center wall of the monolith; as can be seen, the addition of reinforcing has only a slight effect on the resulting stresses. The primary reason that the analysis without reinforcing is so similar to the analysis with reinforcing is that the reinforcing in the walls uses only #9 bars at 12-in. spacing while in the slab two or three rows of #18 bars at 12-in. spacing are included. The multiple layers of #18 bars provide significantly more structural stiffness than the single layer of #9 bars. Even with the large reinforcing bars, differences between the analyses are relatively small and demonstrate that inclusion of reinforcing in uncracked sections does not provide substantial benefits.

## Uncracked Versus Cracked

As noted in the previous discussion, no cracking occurred in the analyses of the chamber monolith; therefore, the full effects of the reinforcing could not be realized. In order to observe the effects of reinforcing when cracking does occur, the cracking criteria were reduced to artificially induce cracking in the monolith. To achieve the decreased cracking criteria, the cracking strain was reduced by a factor of two.

Figures 22-26 are plots comparing an analysis without the crack criteria reduced and an analysis with the reduced crack criteria. The primary crack that formed in the slab began in element 756 as can be seen in Figure 27a which shows the integration points which cracked in the analysis with the reduced cracking criteria. This is very obvious when looking at the results for element 756 as shown in Figure 24 where the stress in the concrete drops to zero at approximately day 130 when the crack first formed. The effects of cracking

can also be observed in the concrete stresses for element 493 (Figure 22) and element 763 (Figure 23) where slight drops in stress occur at the time the crack forms (approximately day 140). While these two points indicate that cracking has occurred, they do not provide definitive information regarding the crack location. The reduction of stress at these points is a result of the crack allowing a reduction in the restraint occurring at the top of the slab, which is in tension. Since thermal stresses in the concrete develop due to restraint, the crack serves to relieve some of this restraint, which in turn reduces the stress.

Figure 25 shows the stress in element 993 in the wall for uncracked and cracked analyses. Since only one integration point cracked, this would indicate that the cracking is small, and therefore the effect on the stresses in the concrete is small. Little difference between the two analyses is observed in Figure 26 since no cracking has occurred in the vicinity of element 1196.

Finally, Figures 28 and 29 show the stresses that result in the reinforcing. As noted previously, and shown in Figure 27, the primary crack in the slab occurred at element 756. The plot of reinforcing stresses in Figure 28 for this element shows how, for the analysis in which cracking occurs, the stresses in the reinforcing increase dramatically. This increase is not seen in areas where cracking does not occur; this fact is demonstrated in Figure 29 for element 763 where the reinforcing stresses actually decrease when the cracking occurs in nearby elements. The reinforcing behaves in the same manner as the concrete in the locations in which there is no cracking. It should also be noted that even though the reinforcing stress in element 756 rises dramatically when cracking occurs, the stresses in the reinforcing are low and indicate that if this were not an induced condition, mitigating measures would not be necessary as a result of this cracking.

## Summary

As can be seen in the results presented comparing the analyses with and without cracking, modeling reinforcing can be effective in its application to analyze massive concrete structures. The first two analyses showed that reinforcing will have only minor effects on the resulting behavior if cracking does not occur.

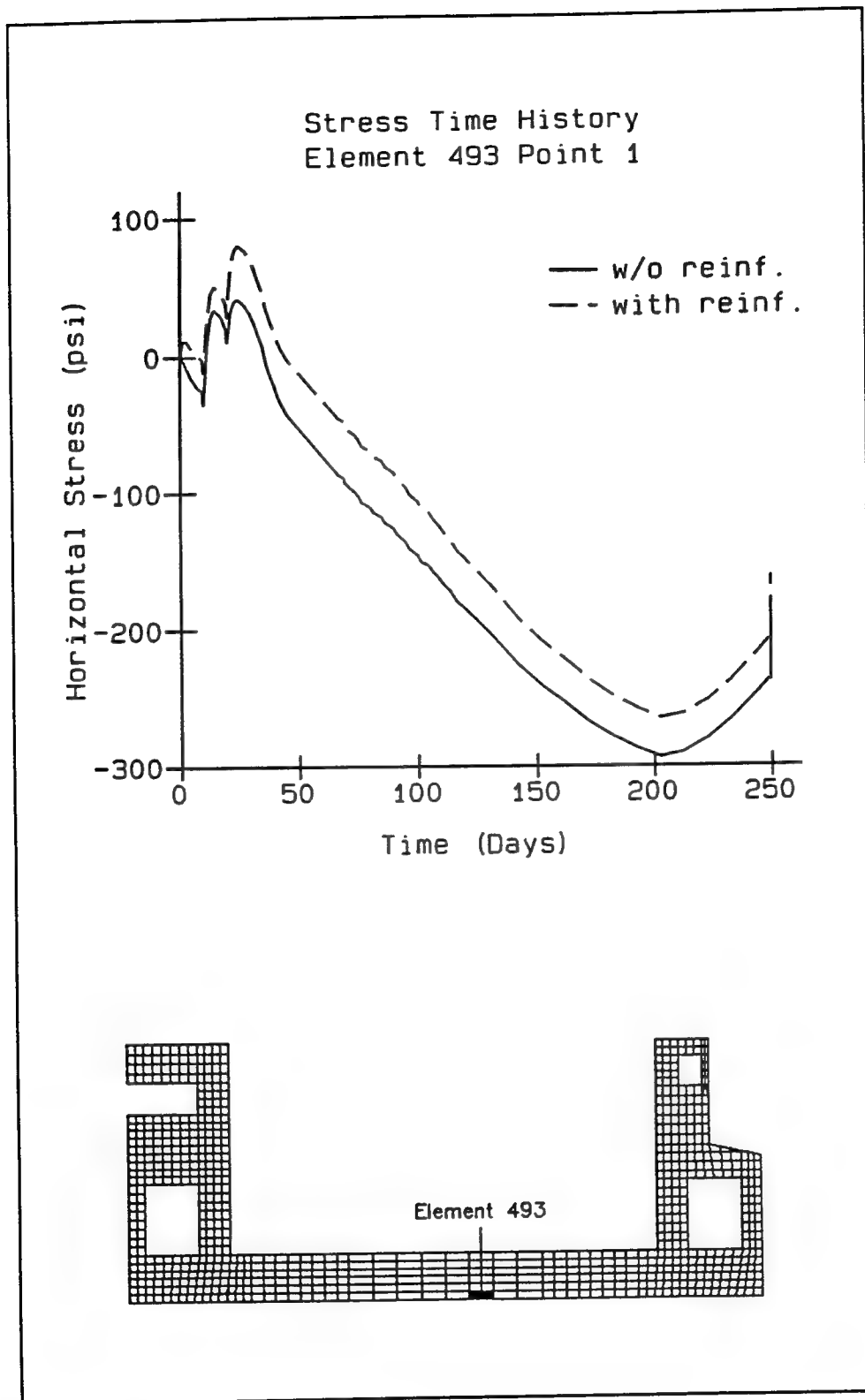


Figure 17. Horizontal stress comparison of reinforced and unreinforced cases for element 493, integration point 1

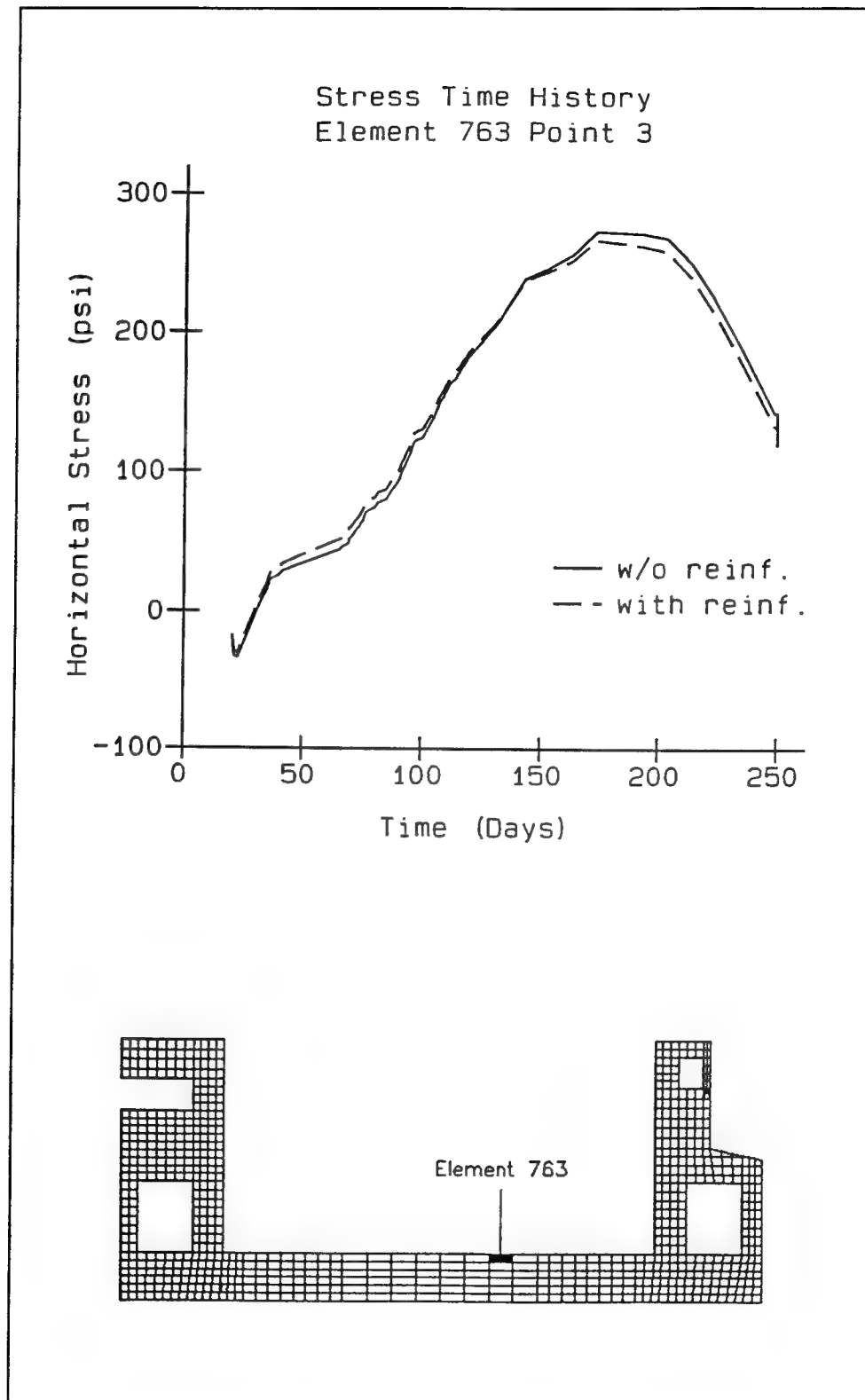


Figure 18. Horizontal stress comparison of reinforced and unreinforced cases for element 763, integration point 3



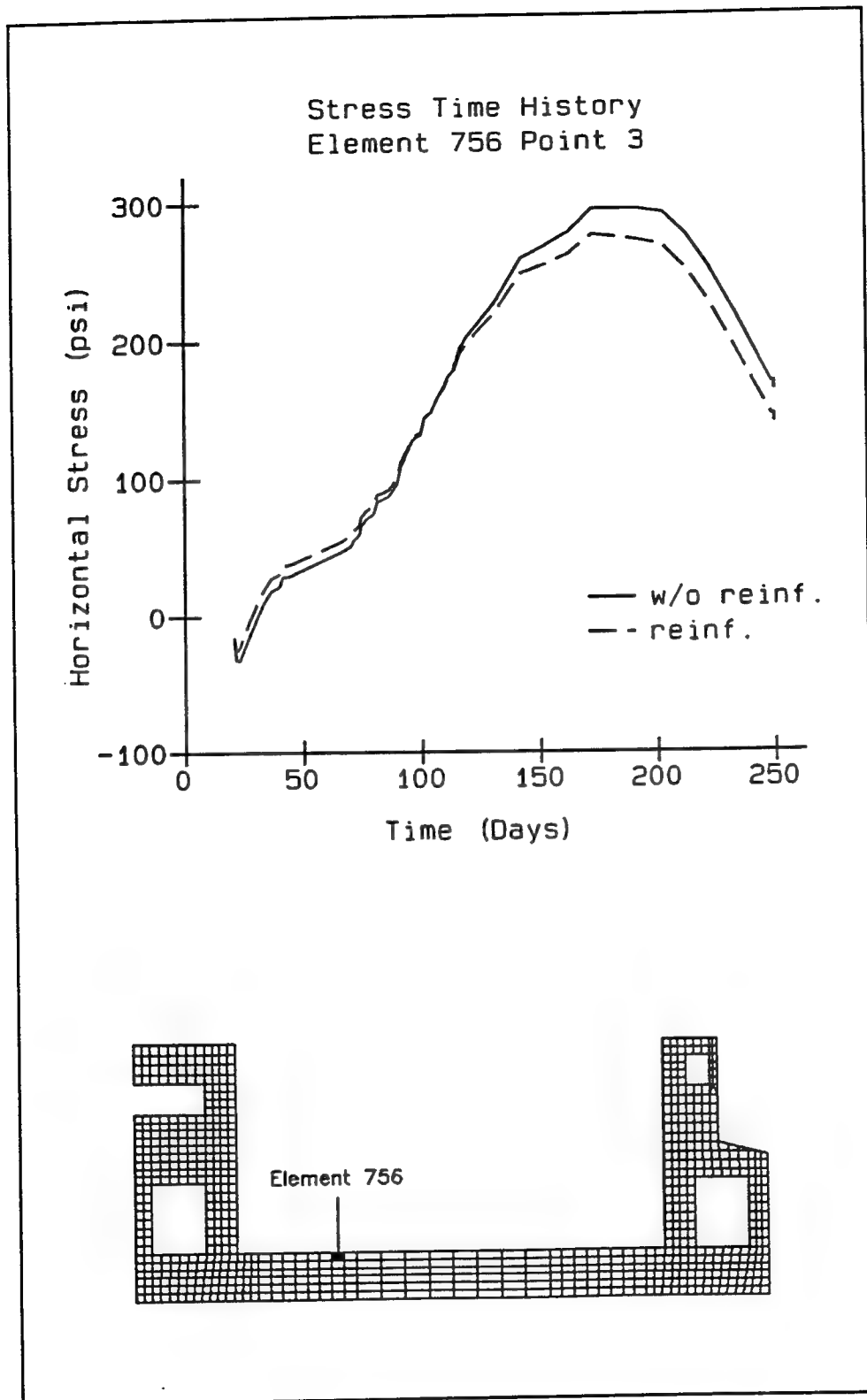


Figure 19. Horizontal stress comparison of reinforced and unreinforced cases for element 756, integration point 3

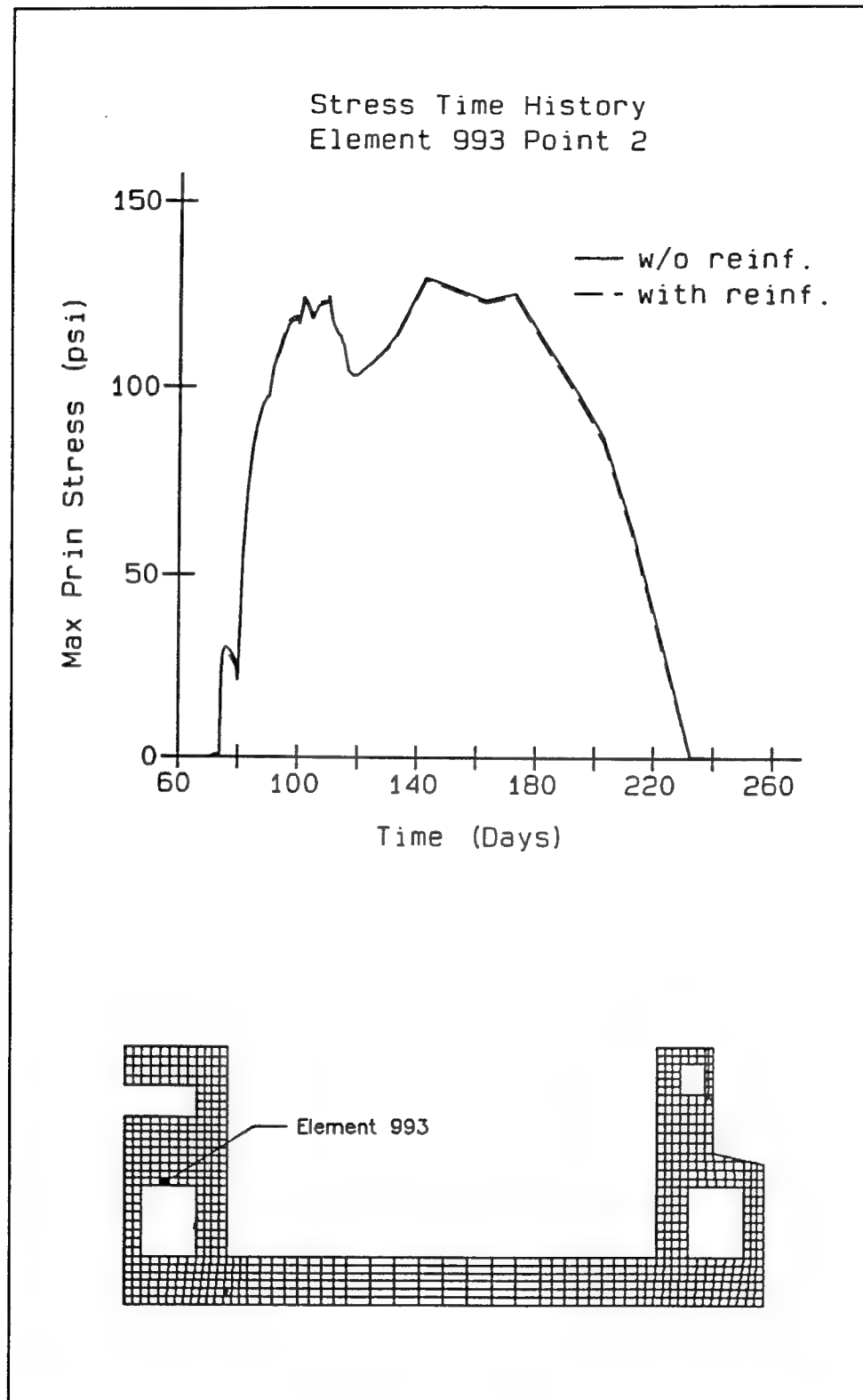


Figure 20. Maximum principal stress comparison of reinforced and unreinforced cases for element 993, integration point 2

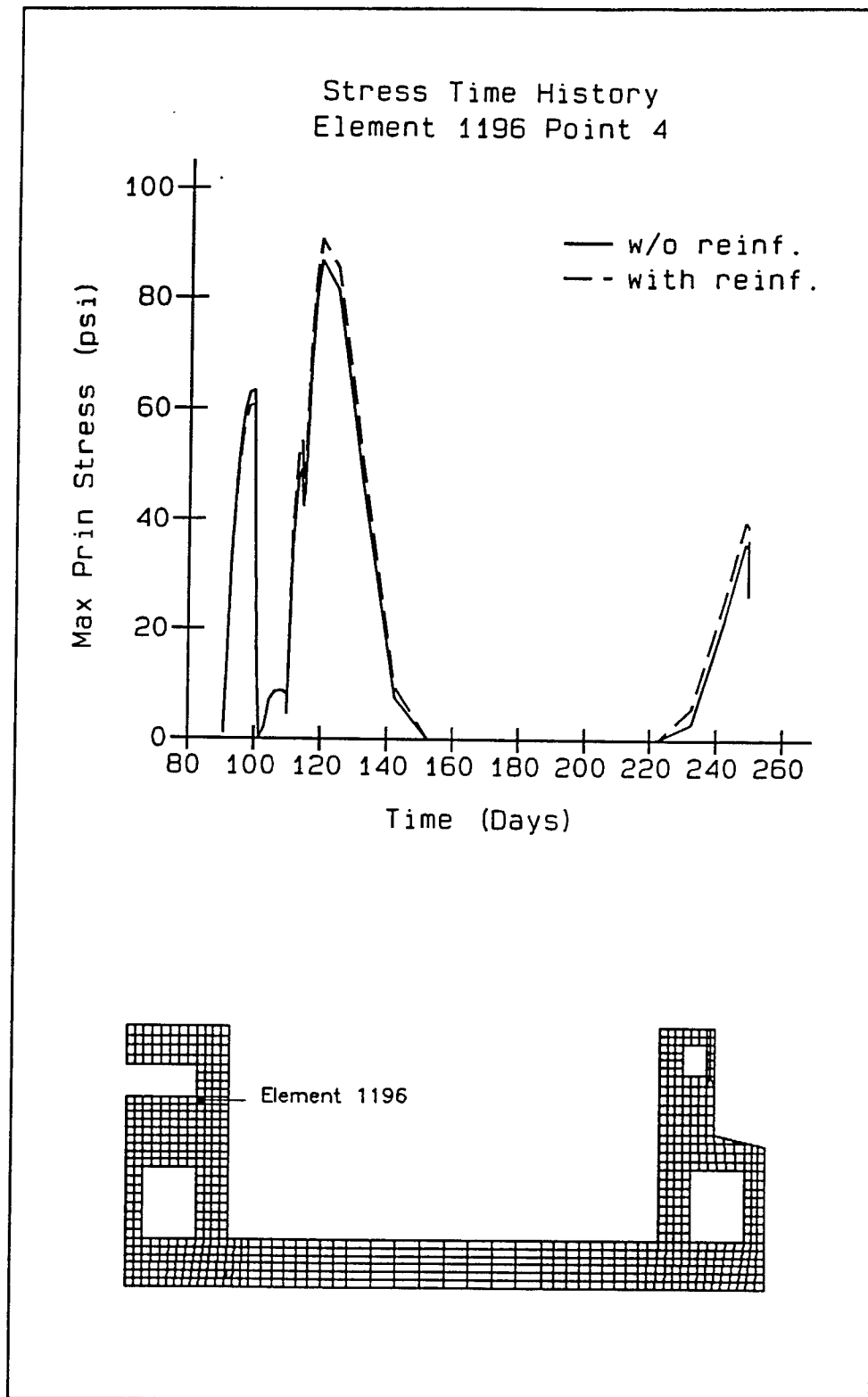


Figure 21. Maximum principal stress comparison of reinforced and unreinforced cases for element 1196, integration point 4

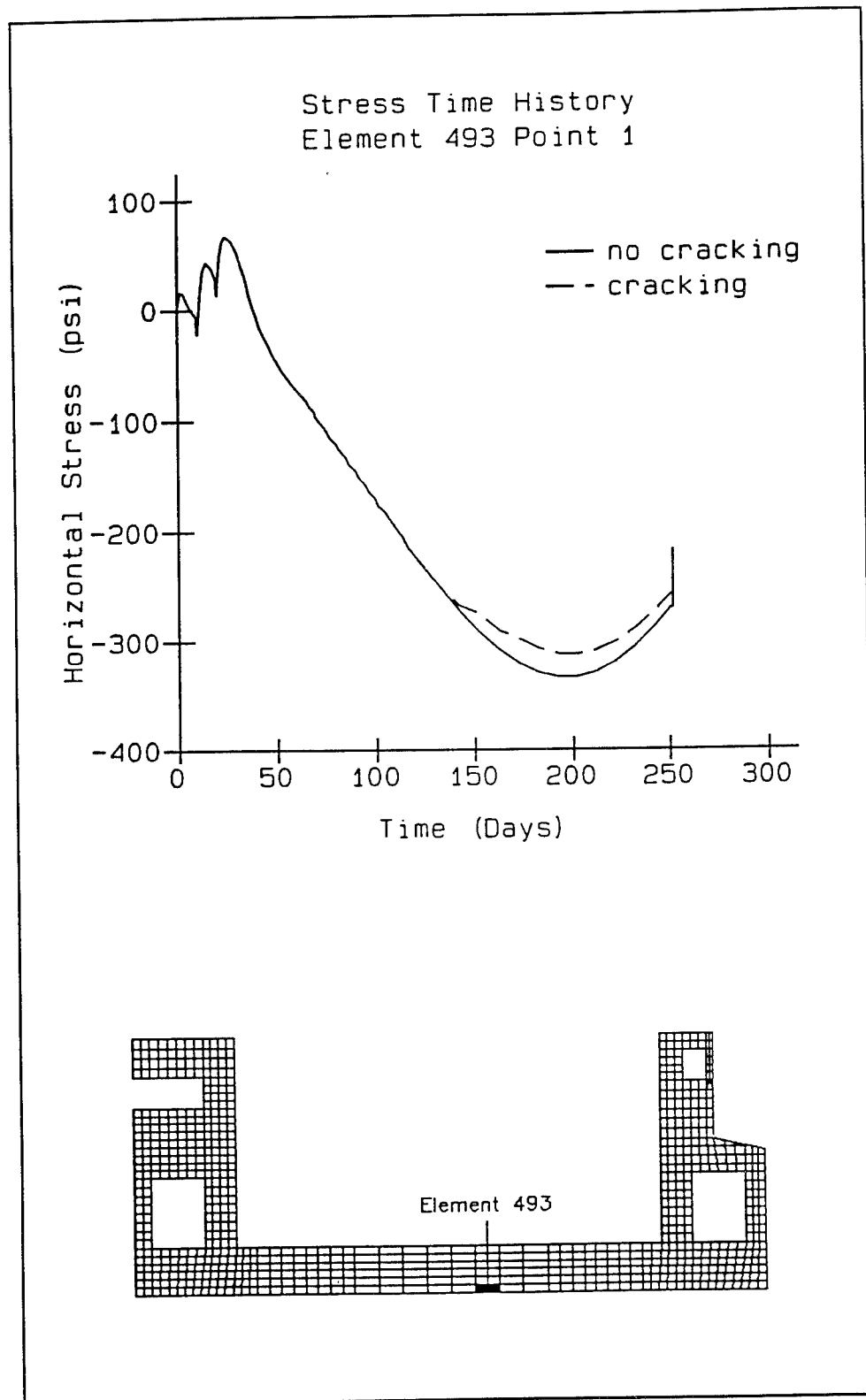


Figure 22. Horizontal stress comparison of cracked and uncracked cases for element 493, integration point 1

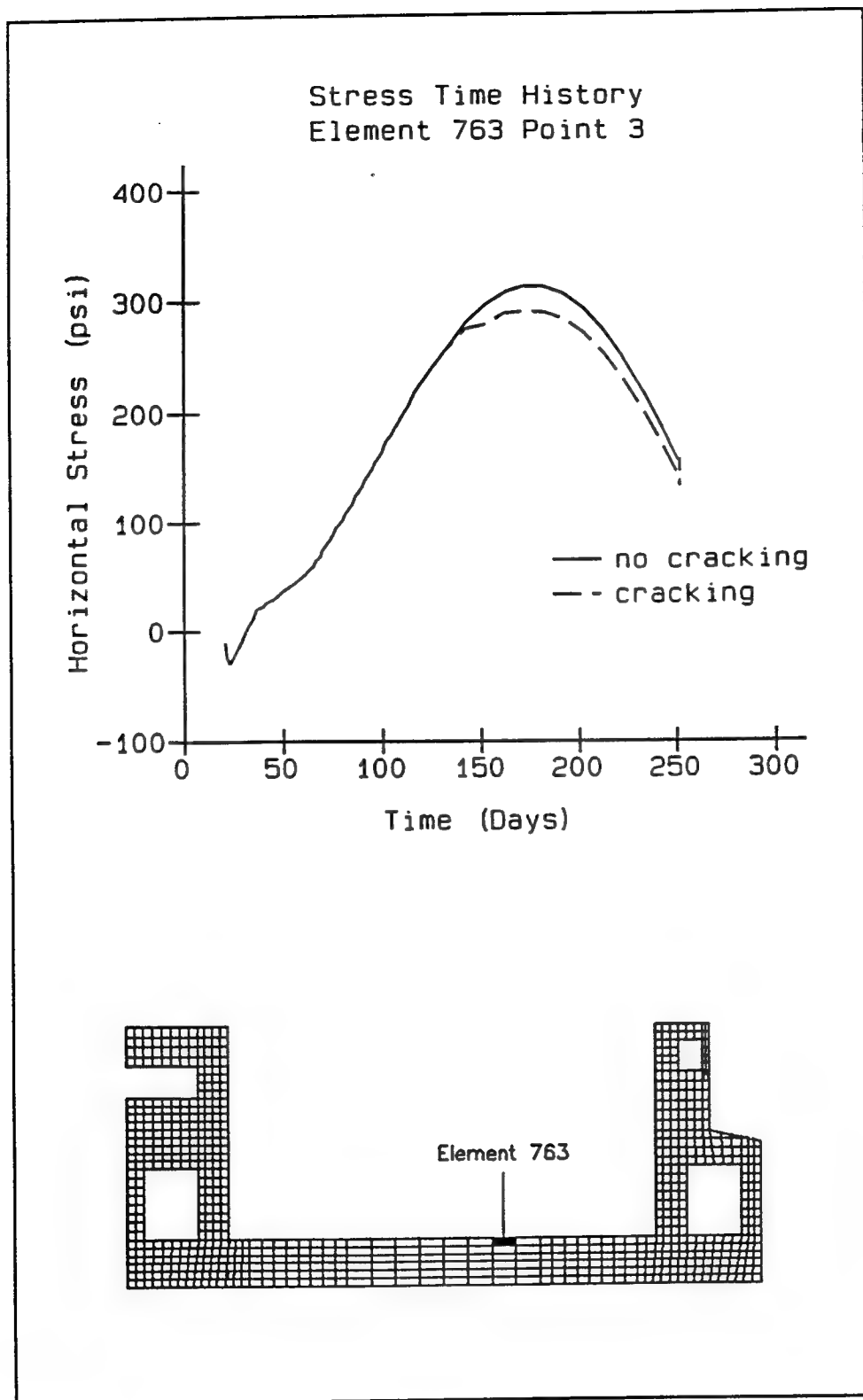


Figure 23. Horizontal stress comparison of cracked and uncracked cases for element 763, integration point 3

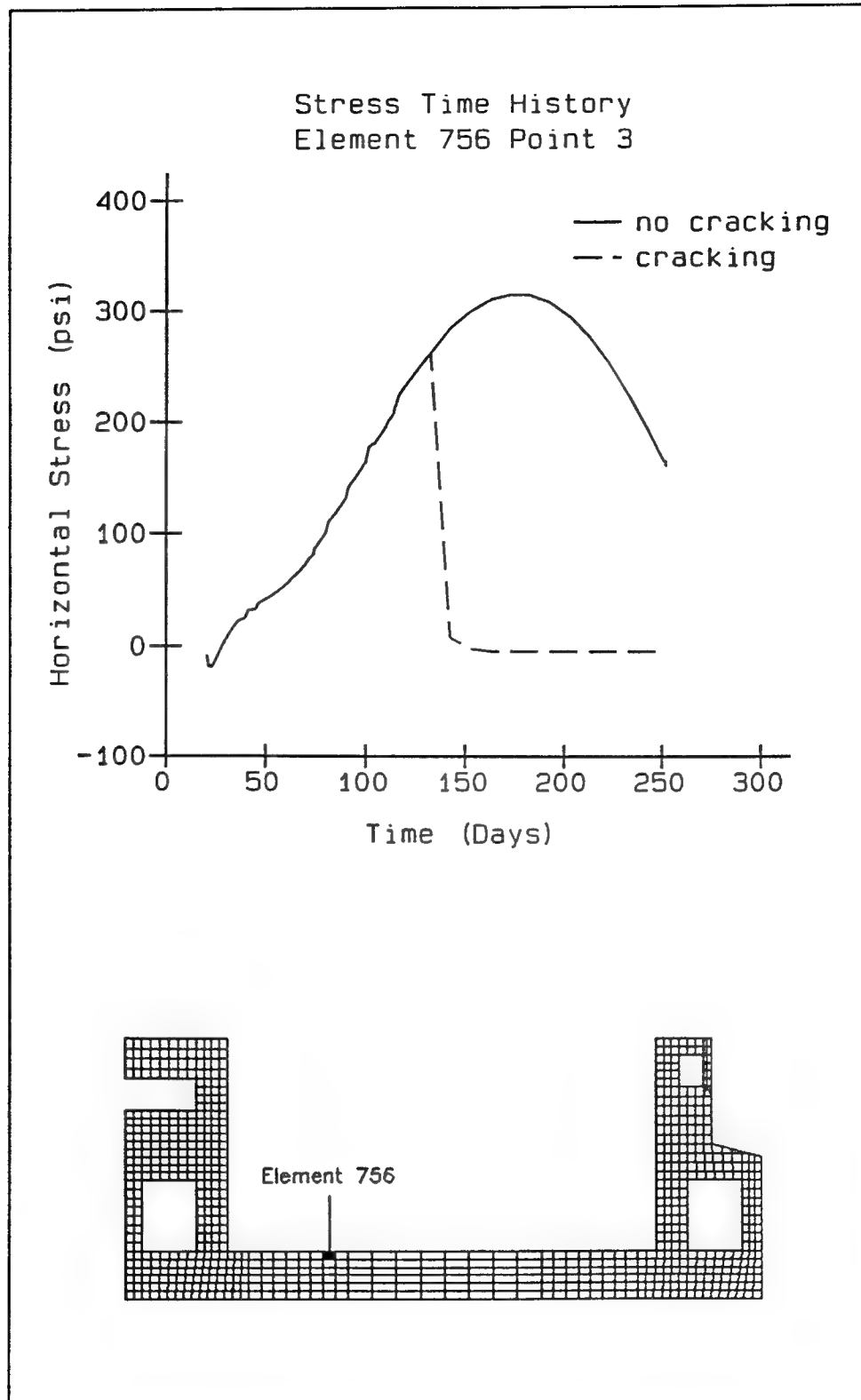


Figure 24. Horizontal stress comparison of cracked and uncracked cases for element 756, integration point 3

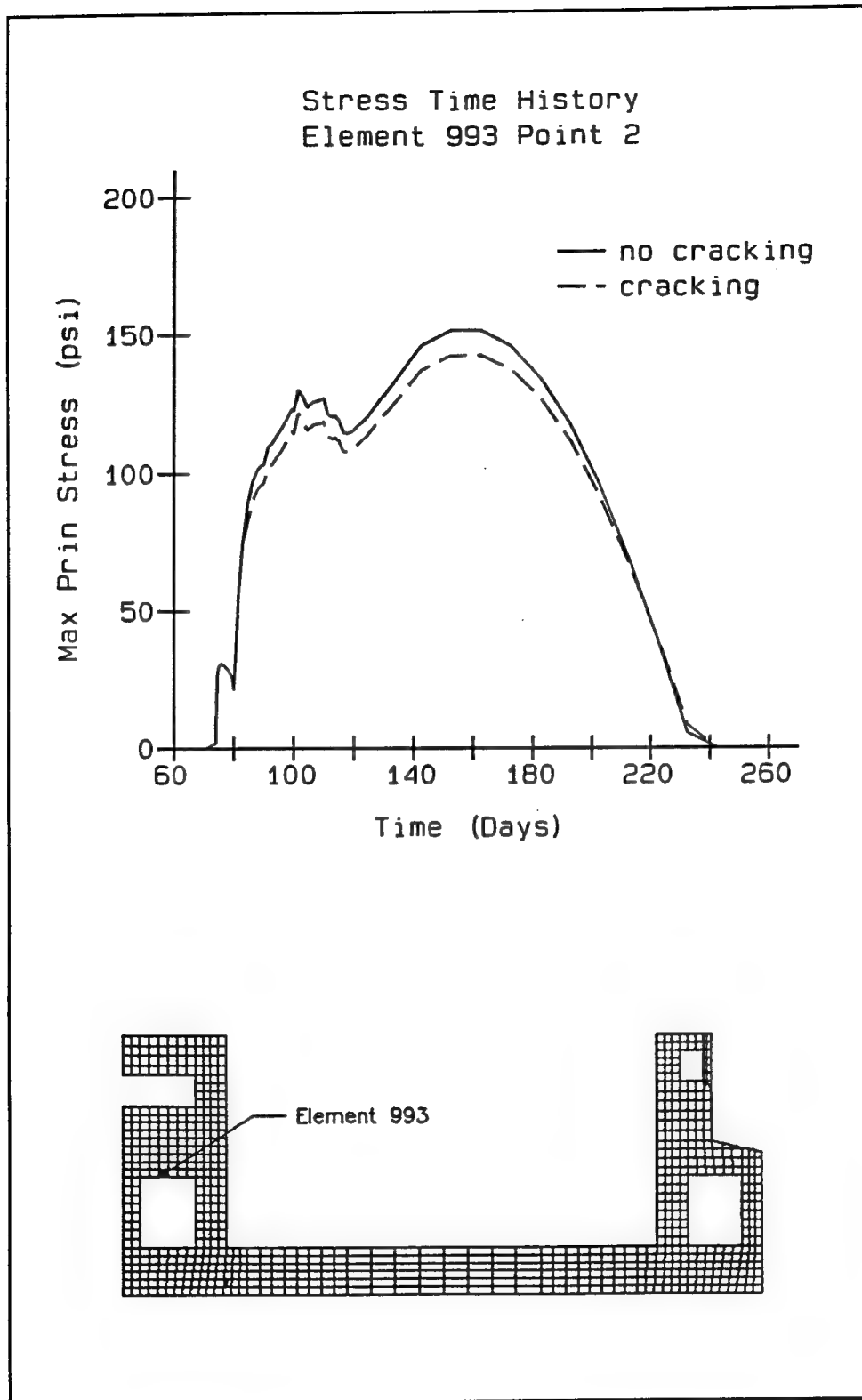


Figure 25. Maximum principal stress comparison of cracked and uncracked cases for element 993, integration point 2

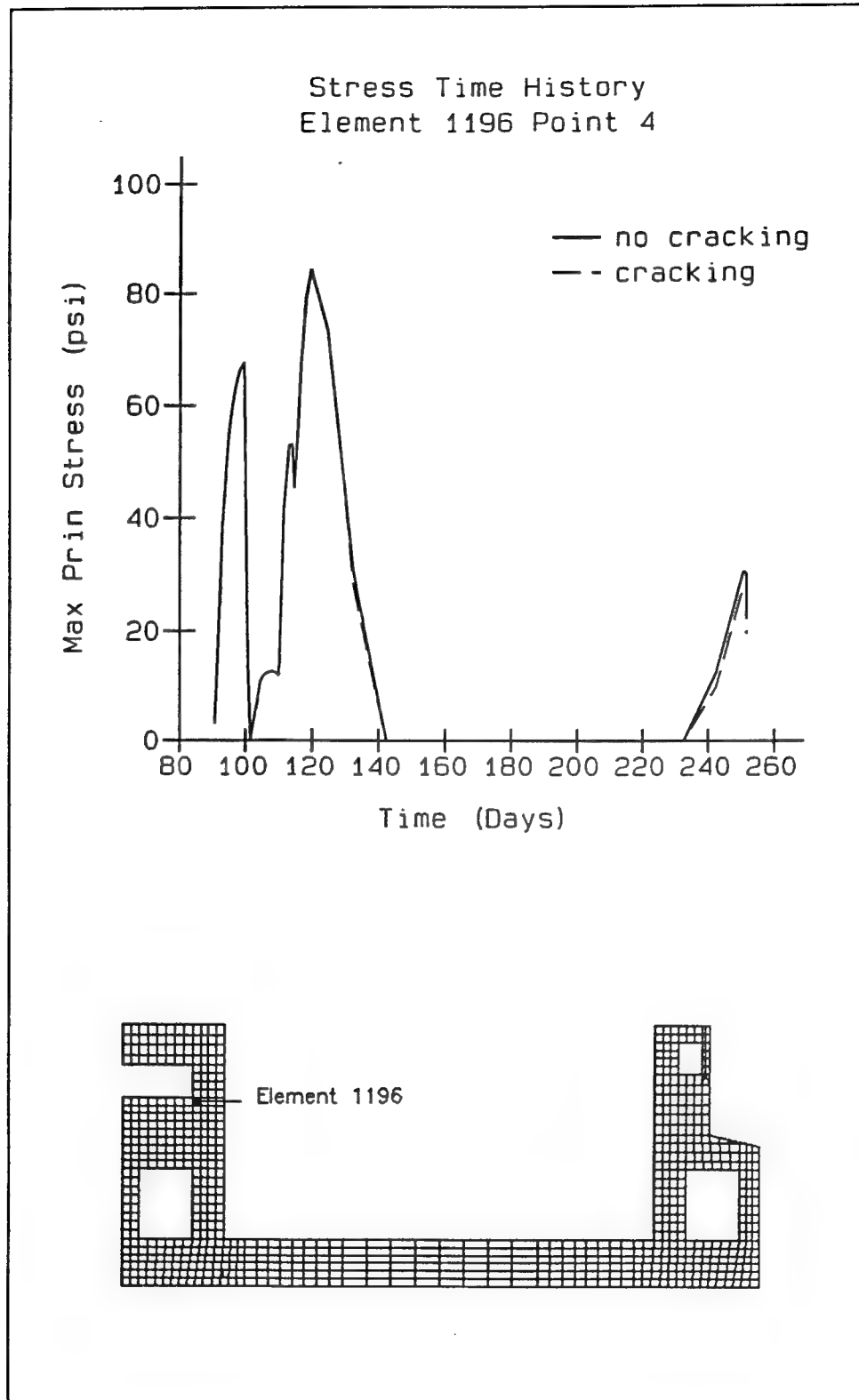


Figure 26. Maximum principal stress comparison of cracked and uncracked cases for element 1196, integration point 4



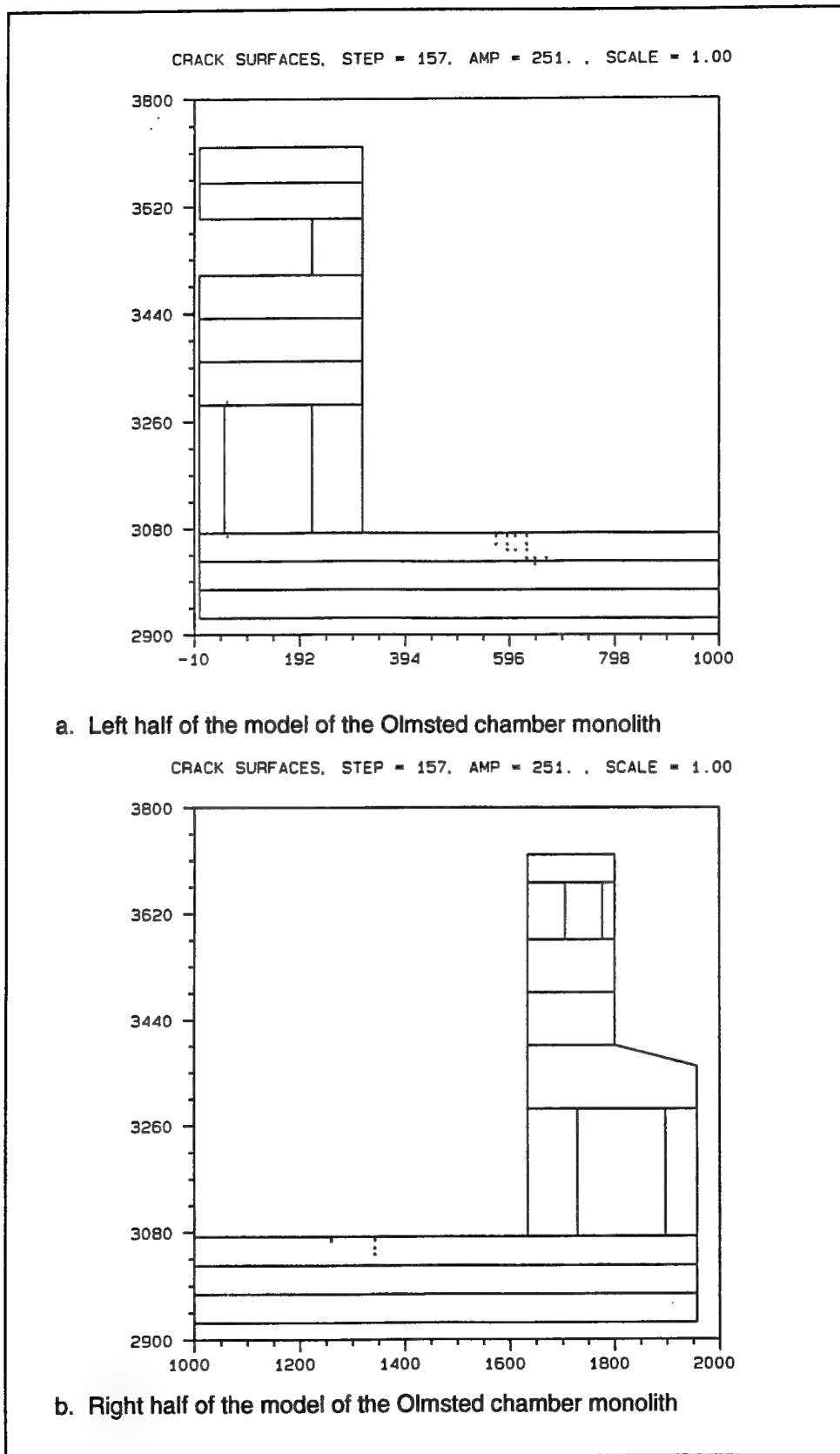


Figure 27. Crack location plots

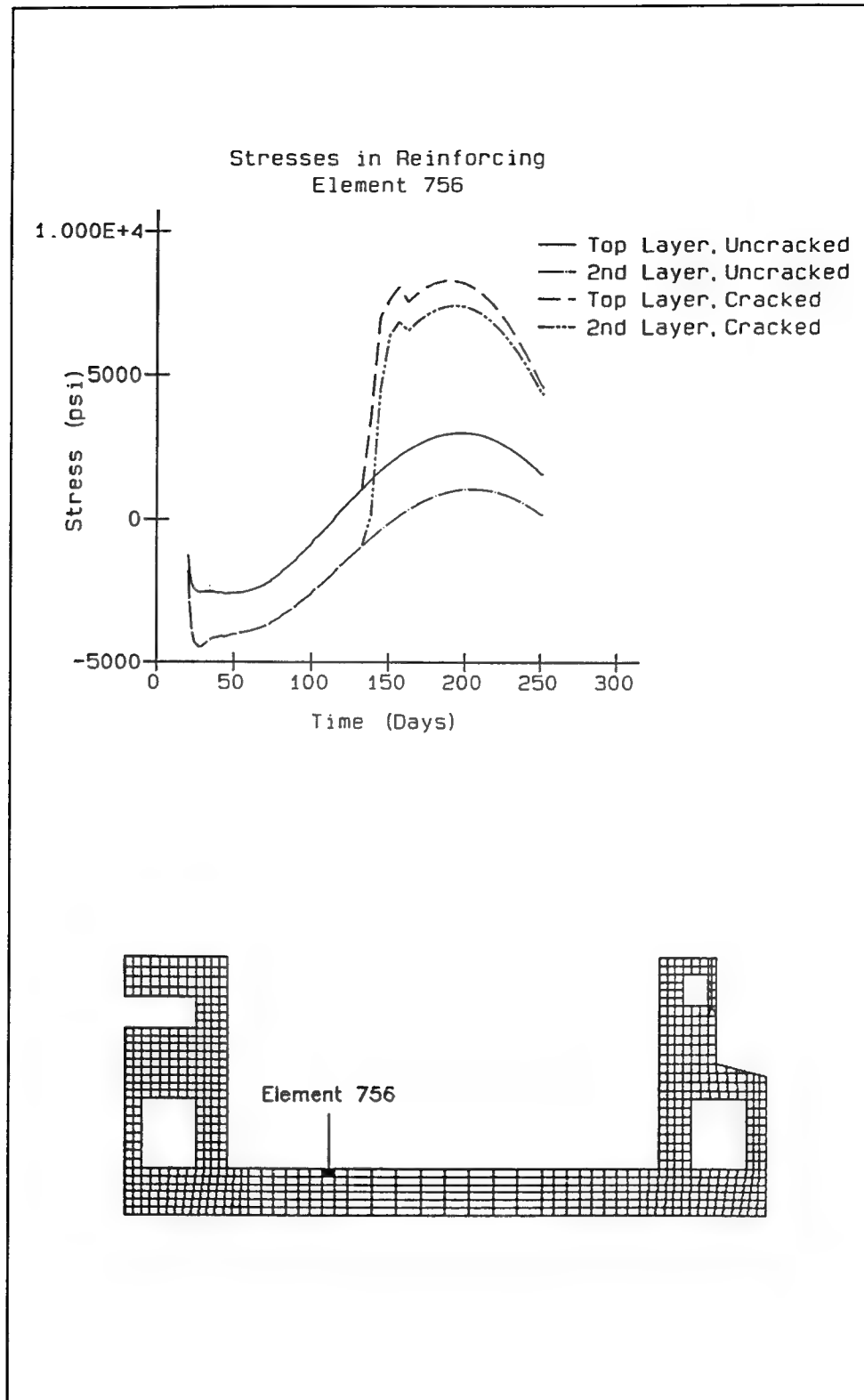


Figure 28. Reinforcing stress comparison of cracked and uncracked cases for element 756

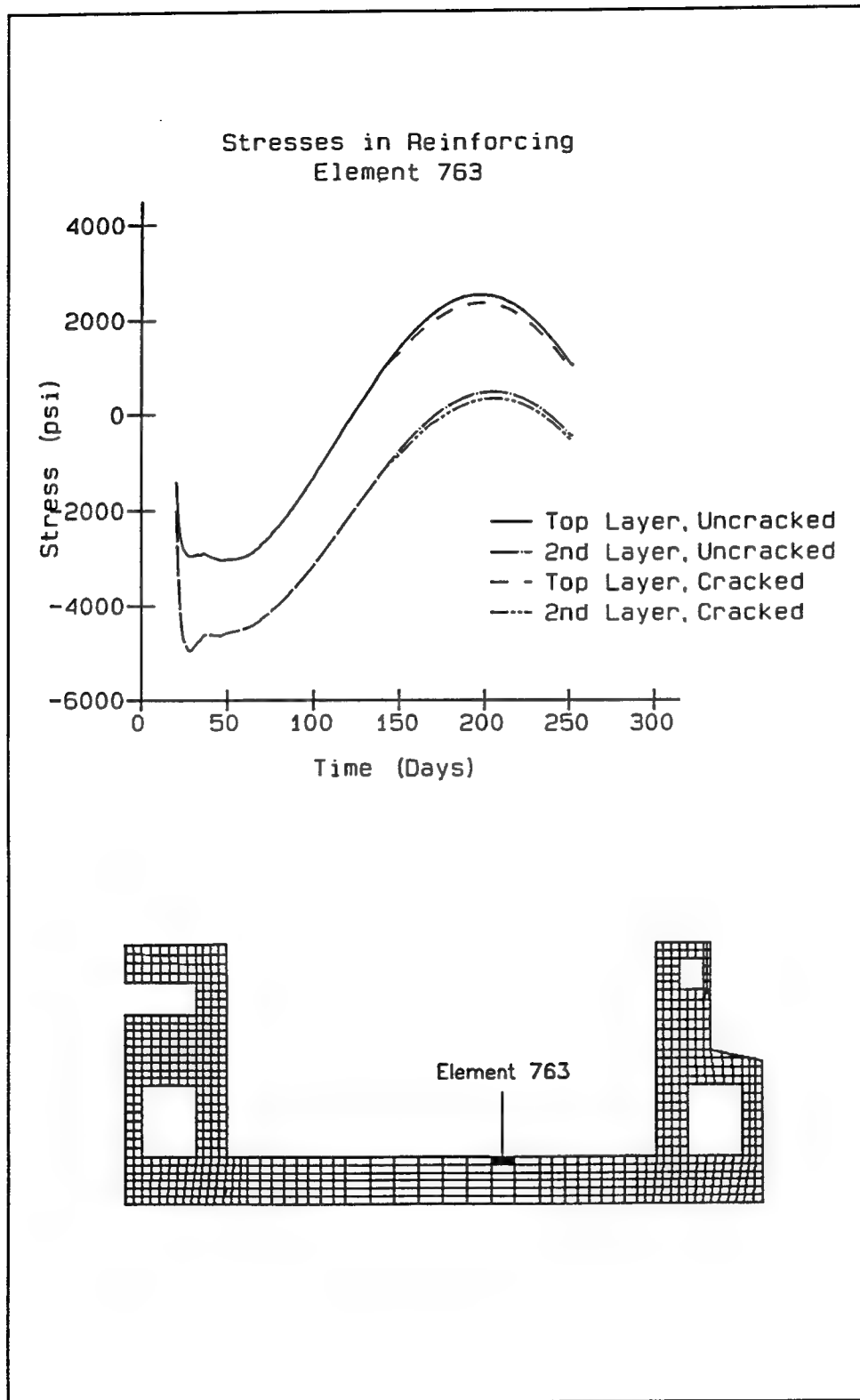


Figure 29. Reinforcing stress comparison of cracked and uncracked cases for element 763

# 6 Summary and Conclusions

---

## Summary

The primary objectives of this report were to provide understanding with respect to the calculation of stresses in reinforcing and to gain confidence in performing finite element analyses which include reinforcing steel. Chapters 2, 3, and 4 provided detailed examinations of stress calculation in the concrete and steel to provide a background on how to compute stresses for various loadings, and once computed, how these calculated values compared to the values provided by a finite element analysis. In each case, agreement between the two methods of calculation was exact or nearly exact.

Analyses of a typical chamber monolith were presented in Chapter 5 to demonstrate how the use of reinforcing in a finite element analysis can be achieved and to show its impact on the results. This example was included to further the understanding associated with modeling reinforcement and to provide confidence for using these techniques in association with massive concrete structures.

Inclusion of reinforcing in a NISA study can be extremely beneficial to the performance of a model. Subsequent to initiation of this study, NISA studies were performed on other massive concrete structures that included reinforcing in the model and which exhibited cracking (Fehl et al., in preparation, and Fehl, Riveros, and Garner, in preparation). In these studies, adjustment of construction parameters did not totally mitigate cracking. Stresses in the reinforcing were evaluated in order to make a determination as to whether the behavior of the structures was satisfactory. The results of these evaluations indicated that stresses in the reinforcement were low and were in areas which were not detrimental to the structural performance; therefore, the minor cracking that did occur was tolerable.

## Conclusions

The examples shown in Chapters 2-5 have shown that modeling of reinforcing in a NISA study is reliable and indeed feasible. Studies in Chapter 2 demonstrated that the REBAR option in ABAQUS may be used to perform this modeling. Results of analyses using the REBAR option were compared to results of analyses using linear truss elements and it was shown that the sets of

results were equivalent. It is recommended that the ABAQUS REBAR option be used in all future NISA studies based on these results. Examples of how to input reinforcing using this option are provided in Appendix A.

The data from the simple problems evaluated in this report also showed how the results from a finite element analysis can be predicted using hand calculation methods. This was demonstrated in Chapters 2 and 3 for mechanical loads and in Chapters 2 and 4 for thermal loads. In addition, the calculations were accomplished for problems with and without reinforcing. Based on these results, it can be concluded that using reinforcing in a NISA study is an acceptable modeling technique and is suitable for use in service load conditions.

Finally, it was also demonstrated that reinforcing is not fully utilized until cracking occurs in the concrete. Results in Chapters 2 and 5 clearly demonstrate that inclusion of reinforcing in the model has a very minor effect on the resulting concrete stresses if no cracking of the concrete occurs and that the stresses in the reinforcing are also very minimal. It was also shown that once cracking of the concrete occurred, there were dramatic increases in the reinforcing stress. Because a NISA is a nonlinear analysis attempting to model actual structural behavior in which cracking is anticipated, attempts should be made to include reinforcing in NISA studies whenever possible. Exclusion of reinforcing from the model of a NISA study will provide a conservative approach, but the full benefits of performing a NISA or the full structural capacity will not be realized.

# References

---

ANATECH Research Corporation. (1992). "ANACAP-U, ANATECH concrete analysis package user's manual, Version 92-2.2," San Diego, CA.

Bombich, A. A., Garner, S., and Norman, C. D. (1991). "Evaluation of parameters affecting thermal stresses in mass concrete," Technical Report SL-91-2, U.S. Army Engineer Waterways Experiment Station, Vicksburg, MS.

Bombich, A. A., Norman, C. D., and Jones, H. W. (1987). "Thermal stress analyses of Mississippi River Lock and Dam 26(R)," Technical Report SL-87-21, U.S. Army Engineer Waterways Experiment Station, Vicksburg, MS.

Fehl, B. D., and Merrill, C. A. "Three-dimensional, nonlinear, incremental structural analysis of a culvert valve monolith wall, Olmsted Locks," in preparation, U.S. Army Engineer Waterways Experiment Station, Vicksburg, MS.

Fehl, B. D., Garner, S. A., James, R. J., Dunham, R. S., and Zhang, L. "Nonlinear, incremental structural analysis for the Lower Miter Gate Monolith at Olmsted Locks and Dam," in preparation, U.S. Army Engineer Waterways Experiment Station, Vicksburg, MS.

Fehl, B. D., Riveros, G. A., and Garner, S. A. "Nonlinear, incremental structural analysis of McAlpine Locks Replacement Project," in preparation, U.S. Army Engineer Waterways Experiment Station, Vicksburg, MS.

Garner, S., Bombich, A. A., Norman, C. D., Merrill, C. A., Fehl, B. D., and Jones, H. W. (1992). "Nonlinear, incremental structural analysis of Olmsted Locks and Dams; Volume I, Main text," Technical Report SL-92-28, U.S. Army Engineer Waterways Experiment Station, Vicksburg, MS.

Garner, S., Hammons, M., and Bombich, A. (1991). "Red River thermal studies, Report 2, Thermal stress analyses," Technical Report SL-90-8, U.S. Army Engineer Waterways Experiment Station, Vicksburg, MS.

Headquarters, U.S. Army Corps of Engineers. (1994). "Nonlinear, incremental structural analysis of massive concrete structures," ETL 1110-2-305, Washington, DC.

- Headquarters, U.S. Army Corps of Engineers. (1990). "Special design provisions for massive concrete structures," ETL 1110-2-324, Washington, DC.
- Hibbitt, Karlsson, and Sorensen, Inc. (1994). *ABAQUS user's manual*, Version 5.4, Providence, RI.
- Jones, H. W. (1992). "Refined stress analysis of Melvin Price Locks and Dam," Technical Report ITL-92-7, U.S. Army Engineer Waterways Experiment Station, Vicksburg, MS.
- Merrill, C. A., Fehl, B. D., and Garner, S. A. (1995). "Nonlinear, incremental structural analysis of Olmsted Locks: Phase III," Technical Report ITL-95-1, U.S. Army Engineer Waterways Experiment Station, Vicksburg, MS.
- Truman, K. Z., Petruska, D., and Ferhi, A. (1992). "Evaluation of thermal and incremental construction effects for Monoliths AL-3 and AL-5 of the Melvin Price Locks and Dams," Contract Report ITL-92-3, U.S. Army Engineer Waterways Experiment Station, Vicksburg, MS.

# Appendix A

## ABAQUS Modeling

---

The discussion in this appendix is provided to assist the reader in modeling reinforcement in a finite element model using the ABAQUS finite element code (Hibbitt, Karlsson, and Sorensen 1994). The information is for the modeling of reinforcing using the \*REBAR option provided by ABAQUS which incorporates the reinforcing into the element stiffness matrix for the element which contains the reinforcing. The methods outlined in this appendix were used in the models discussed in the main body of the report.

It should be noted that the methods for using reinforcing as discussed in this report were developed for incorporation of NISA studies, but these same modeling techniques may be used in other types of analyses should the designer find an area outside of NISA where modeling reinforcement may be beneficial. One possible application of using reinforcing in a finite element model is in a dynamic analysis.

A discussion of the \*REBAR option may be found in the ABAQUS user's manual (Hibbitt, Karlsson, and Sorensen 1994) in section 7.4.6. As discussed in the user's manual, two parameters must be included with the \*REBAR option: ELEMENT and MATERIAL. For NISA studies, the ELEMENT parameter should be set equal to CONTINUUM for both two-dimensional (2-D) and 3-D studies. The MATERIAL parameter must be set equal to the name given on the material card where the properties of the reinforcing are provided. Examples will be shown further in this discussion.

Other parameters which may be included with the \*REBAR option are the GEOMETRY, NAME, and SINGLE parameters. If reinforcing is orthogonal and parallel to element sides, then the GEOMETRY parameter can be ignored since this is the default setting. If reinforcing is not parallel to element sides, then the GEOMETRY parameter should be set equal to SKEW. The NAME parameter does not have to be specified, but since this identifier can be used to define output for the reinforcing, it should generally be included. The SINGLE parameter is used only if one reinforcing bar is being defined as opposed to a layer of bars. This parameter will usually not be needed in NISA studies.

The \*REBAR option card may appear as follows in the input file of finite element model containing reinforcement:



```
*REBAR,ELEMENT=CONTINUUM,MATERIAL=STEEL,GEOMETRY
=SKEW,NAME=REINF
```

This definition would be for a 2-D or 3-D analysis using continuum-type elements, and the name of the material definition for the reinforcing is STEEL. The bars do not have to be parallel to element sides, and the name assigned to the reinforcing being defined is REINF.

For the \*REBAR option card shown above, since GEOMETRY=SKEW was defined, then two lines of data must follow. For 2-D analyses four items must be included in the first line of data. The first piece of data is the element number containing the reinforcing or the element set name of the elements containing the reinforcing. The second piece of data is the cross-sectional area of the reinforcing bar followed by the spacing of the bars. Finally, the orientation of the bars must be defined giving the angle in degrees between the local axis and the orientation of the bars. Figure A1 shows the orientation angle. If a 3-D analysis is being performed, the user should input two commas after the bar orientation definition followed by the isoparametric direction.

The second line of data contains the fractional distances along the edges of the element where the reinforcing bars intersect the side of the element as shown

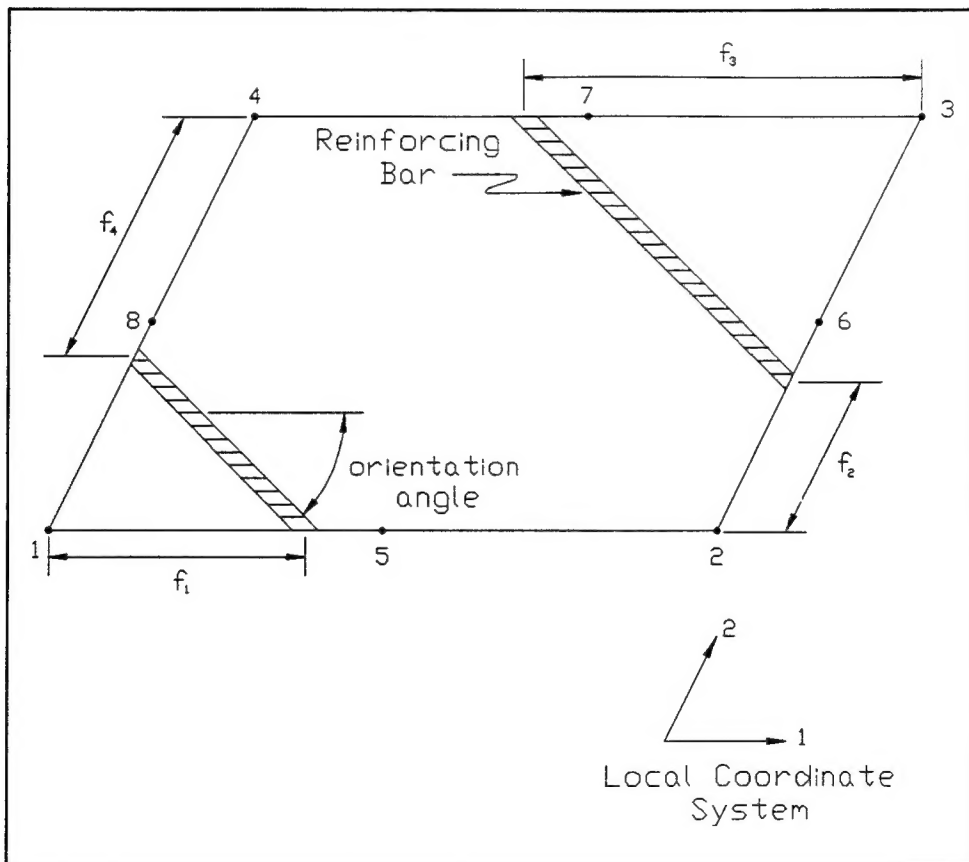


Figure A1. Notations for identifying skewed reinforcement in an ABAQUS, eight-noded isoparametric element

in Figure A1. Descriptions of these fractional distances are given in the ABAQUS user's manual.

The two lines of data following the \*REBAR option card may look like the following:

```
BARS,1.0,12.0,0.0,,1
0.0,0.5,0.0,0.5
```

The lines define a set of elements called BARS which contain the reinforcing bars. The bar size is 1.0 in.<sup>2</sup> (#9 bar) spaced at 12 in. The orientation of the bars is 0.0 deg, and if a 3-D analysis is being performed, the isoparametric direction is in the direction of the first axis (typically x). The second line defines the bar intersecting the sides of the elements in element set BARS at a point half way up on side 2 of the element and half way down on side 4 of the element as shown in Figure A2.

Alternatively, if the GEOMETRY parameter is not included or is set equal to ISOPARAMETRIC, only one additional line is required to define the bars. The first four pieces of data are identical to the first four pieces of data defined in the first line of data given above. For the ISOPARAMETRIC definition, the fractional distance from the defined edge is given after the orientation followed by the defined edge. If the analysis is 3-D, then the isoparametric directions must be given after defining the edge.

As an example, consider the cantilevered beam used in Chapter 2 as the illustration for the example problem. For one of the analyses performed in Chapter 2, a single reinforcing bar was placed at the center of the beam for the length of the beam. For this problem there were six elements contained in an

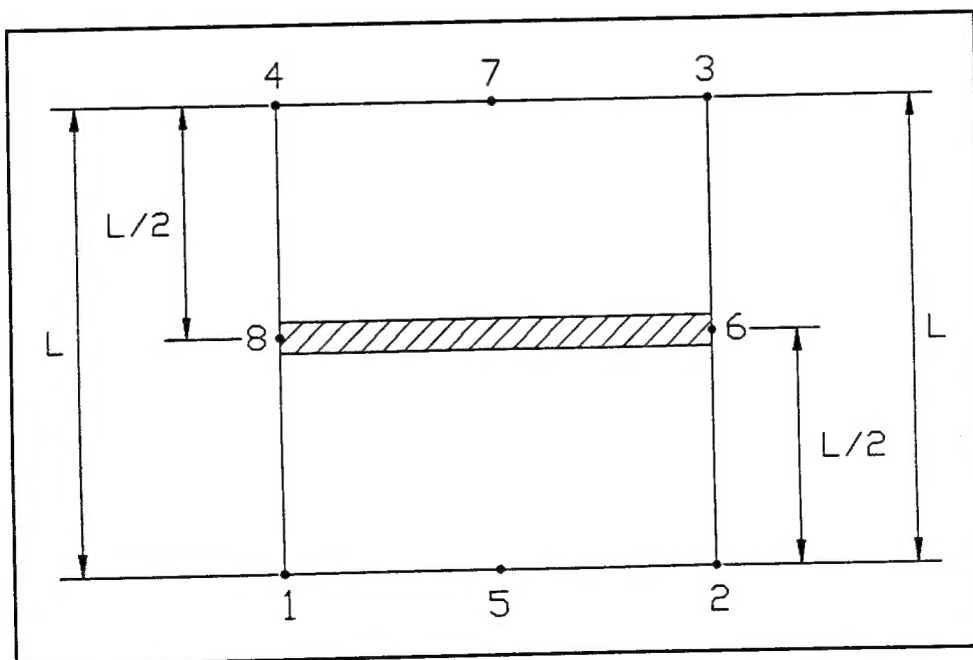


Figure A2. Location of a reinforcing bar at midheight of an element

element set called ALL, the reinforcing steel was assigned to a material called STEEL, and the material definition in the input file was given as follows:

```
*MATERIAL,NAME=STEEL
*DENSITY
0.2836
*ELASTIC
29.0E6,0.3
*EXPANSION
6.5E-6
```

The bar used in the problem was a #9 bar ( $A_s = 1.0 \text{ in.}^2$ ) at 12-in. spacing. Given this information, the reinforcing bar was specified with the \*REBAR option in ABAQUS. The default value of ISOPARAMETRIC was used for the GEOMETRY parameter and the input was given by:

```
*REBAR,ELEMENT=CONTINUUM,MATERIAL=STEEL,NAME=REINF
ALL,1.0,12.0,0.0,0.5,1
```

As can be seen, the reinforcing defined was assigned to the group REINF. If the GEOMETRY parameter is set equal to SKEW, then the same bar can be defined by:

```
*REBAR,ELEMENT=CONTINUUM,MATERIAL=STEEL,GEOMETRY
=SKEW,NAME=REINF
ALL,1.0,12.0,0.0
0.0,0.5,0.0,0.5
```

To obtain results for the reinforcing (e.g., stresses) for the example shown above, the user must include the following lines in the input file during the step definition:

```
*EL FILE,ELSET=ALL,REBAR=REINF
S
```

This will provide results of the stresses in the reinforcing for the bars in element set ALL in a binary file. If the results are desired in an ASCII file, then the \*EL FILE option should be changed to the \*EL PRINT option.

The above discussion and example demonstrate how the user can input reinforcing into a finite element model. Preprocessors also exist which can assist in the placement of the reinforcing. One of these preprocessors is part of the ANACAP-U software (ANATECH Research Corp. 1992). Contained within the ANACAP-U software is a preprocessor called ANAGEN. If ANAGEN is used to generate the finite element mesh, then the reinforcing can be included in the model by simply identifying the end coordinates of the reinforcing bars, and giving the area of steel and the spacing of the reinforcing. Given this information, ANAGEN will automatically generate the input associated with the \*REBAR option. If reinforcing is not completely orthogonal, the user should consider using a preprocessor such as ANAGEN to avoid input errors.

# REPORT DOCUMENTATION PAGE

Form Approved  
OMB No. 0704-0188

Public reporting burden for this collection of information is estimated to average 1 hour per response, including the time for reviewing instructions, searching existing data sources, gathering and maintaining the data needed, and completing and reviewing the collection of information. Send comments regarding this burden estimate or any other aspect of this collection of information, including suggestions for reducing this burden, to Washington Headquarters Services, Directorate for Information Operations and Reports, 1215 Jefferson Davis Highway, Suite 1204, Arlington, VA 22202-4302, and to the Office of Management and Budget, Paperwork Reduction Project (0704-0188), Washington, DC 20503.

<b>1.AGENCY USE ONLY (Leave blank)</b>		<b>2.REPORT DATE</b> September 1995	<b>3.REPORT TYPE AND DATES COVERED</b> Final report	
<b>4.TITLE AND SUBTITLE</b> Use of Reinforcement in a Nonlinear, Incremental Structural Analysis			<b>5.FUNDING NUMBERS</b>	
<b>6.AUTHOR(S)</b> Barry D. Fehl, Chris A. Merrill				
<b>7.PERFORMING ORGANIZATION NAME(S) AND ADDRESS(ES)</b> U.S. Army Engineer Waterways Experiment Station 3909 Halls Ferry Road Vicksburg, MS 39180-6199			<b>8.PERFORMING ORGANIZATION REPORT NUMBER</b> Technical Report ITL-95-7	
<b>9.SPONSORING/MONITORING AGENCY NAME(S) AND ADDRESS(ES)</b> U.S. Army Corps of Engineers Washington, DC 20314-1000			<b>10.SPONSORING/MONITORING AGENCY REPORT NUMBER</b>	
<b>11.SUPPLEMENTARY NOTES</b> Available from National Technical Information Service, 5285 Port Royal Road, Springfield, VA 22161.				
<b>12a.DISTRIBUTION/AVAILABILITY STATEMENT</b> Approved for public release; distribution is unlimited.			<b>12b.DISTRIBUTION CODE</b>	
<b>13.ABSTRACT (Maximum 200 words)</b> <p>This report discusses the modeling of reinforcement in a finite element method known as nonlinear, incremental structural analysis (NISA). Several simple problems are used to show how reinforcement may be included in a finite element analysis. The problems include an axially loaded beam, a simply supported beam in bending, and a fully supported slab. Closed form solutions for each of the problems are demonstrated.</p> <p>After the theory for each of the simple problems has been presented, example problems are provided to show how the equations are used. The hand calculations are compared to results obtained from finite element analyses. Agreement between hand calculations and numerical results proved to be very good.</p> <p>The report concludes with an example of a NISA performed on a full-scale massive concrete structure. It is concluded that reinforcement is valuable to include in a model if cracking may be expected, but it does not provide significant benefits unless cracking actually occurs.</p>				
<b>14.SUBJECT TERMS</b>  Finite elements Massive concrete  Nonlinear analysis Reinforcing steel			<b>15.NUMBER OF PAGES</b> 74	
			<b>16.PRICE CODE</b>	
<b>17.SECURITY CLASSIFICATION OF REPORT</b> UNCLASSIFIED	<b>18.SECURITY CLASSIFICATION OF THIS PAGE</b> UNCLASSIFIED	<b>19.SECURITY CLASSIFICATION OF ABSTRACT</b>	<b>20.LIMITATION OF ABSTRACT</b>	